

CrossMark  
click for updatesCite this: *J. Anal. At. Spectrom.*, 2017, **32**, 1660Received 8th January 2017  
Accepted 17th February 2017

DOI: 10.1039/c7ja00010c

rsc.li/jaas

## Overcoming spectral overlap via inductively coupled plasma-tandem mass spectrometry (ICP-MS/MS). A tutorial review

Eduardo Bolea-Fernandez,<sup>\*a</sup> Lieve Balcaen,<sup>a</sup> Martin Resano<sup>b</sup> and Frank Vanhaecke<sup>a</sup>

This work reviews the operating principles of ICP-tandem mass spectrometry (ICP-MS/MS) and the key applications reported on since the introduction of the technique in 2012. The main differences between single quadrupole ICP-MS and ICP-MS/MS are elucidated and the tools available for method development are addressed. Examples of real-life applications are given to demonstrate the capabilities of this novel setup in the context of elemental, speciation and isotopic analysis. Attention has been paid to the different approaches (on-mass and mass-shift) allowing interference-free conditions to be obtained.

### 1. Introduction

Inductively coupled plasma-mass spectrometry (ICP-MS) probably is the most powerful technique for obtaining information on the concentration and isotopic composition of the majority of elements in the most diverse sample matrices. However, since its commercial introduction in 1983, the scientific community was also aware of the drawbacks affecting ICP-MS, the occurrence of spectral overlap being a major one.<sup>1–3</sup> Over the years, strong efforts from both academics and

manufacturers have led to the development of different approaches that enable eliminating, or at least mitigating, spectral interferences. Unfortunately, none of these approaches can be considered as universally applicable for interference-free analysis by means of ICP-MS. Although a review of these approaches can be considered to be beyond the scope of this review, it is important to provide a brief overview on the different currently existing options to deal with spectral overlap, aiming at better identifying those situations for which tandem ICP-mass spectrometry (ICP-MS/MS) can be considered of particular interest.

Among the different options to deal with spectral interference, analyte/matrix separation, mathematical equations, and alternative sample introduction approaches, such as vapor

<sup>a</sup>Ghent University, Department of Analytical Chemistry, Campus Sterre, Krijgslaan 281-S12, 9000 Ghent, Belgium. E-mail: Eduardo.BoleaFernandez@UGent.be

<sup>b</sup>University of Zaragoza, Aragón Institute of Engineering Research (I3A), Department of Analytical Chemistry, Pedro Cerbuna 12, 50009 Zaragoza, Spain



Eduardo Bolea Fernández obtained his degree in Chemistry at the University of Zaragoza (Spain) in 2012. After obtaining a Master degree in Analytical Chemistry from the same university, he is currently a PhD student at the Department of Analytical Chemistry, Ghent University (Belgium) in the “Atomic & Mass Spectrometry – A&MS research group”. His research has been focused on

method development for ultra-trace elemental and isotopic analysis using tandem ICP-mass spectrometry (ICP-MS/MS). A second topic of interest is high-precision Hg isotopic analysis using multi-collector ICP-MS. The public defense of his PhD is planned for April 2017.



Lieve Balcaen (1978) obtained her PhD degree in 2005 from Ghent University, Belgium. Until now, she continued carrying out scientific research as a post-doctoral fellow at the same university. Her work focuses on the determination, speciation and isotopic analysis of (trace) elements via ICP-mass spectrometry (ICP-MS). Nowadays, specific topics of research include the development of

analytical methods for ultra-trace determination by means of ICP-tandem mass spectrometry and of speciation strategies based on HPLC-ICP-MS in cooperation with the pharmaceutical industry. Lieve is (co)author of 55 journal papers and 2 book chapters.

generation systems,<sup>4,5</sup> have been used since the early years, in spite of their accompanying drawbacks, such as, lower sample throughput, added labor-intensiveness, loss of multi-element capabilities and/or higher level of uncertainty accompanying the measurement results. The introduction of cool plasma conditions, under which the signals for all Ar-containing ions are strongly decreased, was a first step towards a more general strategy, although this approach was also characterized by important limitations, such as a reduced element coverage, owing to the poor ionization efficiency for elements with a high ionization energy, stronger matrix effects and an enhanced presence of other types of interfering ions (*e.g.*, oxide ions).<sup>6</sup> The introduction of high-resolution (HR) sector-field ICP-MS (SF-ICP-MS) should be considered a crucial breakthrough in this context.<sup>7</sup> However, the increase in mass resolution is accompanied by a significant drop in ion transmission efficiency, and thus in sensitivity (1–2 orders of magnitude), while also a fraction of the interferences (*e.g.*, overlap of the signals from isobaric nuclides) cannot be overcome by using higher mass resolution.<sup>8,9</sup> Furthermore, SF-ICP-MS instrumentation is still more expensive than quadrupole-based ICP-MS (ICP-QMS) instrumentation.

Despite successful demonstration of the capabilities of the use of a collision-reaction cell (CRC) system to overcome spectral overlap by Rowan and Houk in 1989,<sup>10</sup> it was only in the second half of the 1990s that manufacturers started to equip quadrupole-based ICP-MS (ICP-QMS) instruments with such a CRC system. For the first time, ICP-QMS could be considered a competitive approach to SF-ICP-MS for many demanding applications.<sup>11</sup> The introduction of CRCs in ICP-QMS instrumentation (ICP-CRC-QMS) enabled various approaches to avoid spectral overlap by means of control over the collisions and reactions taking place in the cell, thus improving the selectivity of the technique.<sup>12,13</sup> In this way, analyte and interfering ions with the same (nominal) mass-to-charge ( $m/z$ ) ratio could be separated from one another *via* gas

phase ion–molecule processes.<sup>14</sup> This approach is sometimes termed chemical resolution. Non-reactive gases (*e.g.*, He) in combination with kinetic energy discrimination (KED) could be used to reduce the interferences produced by polyatomic ions.<sup>15</sup> These ions show a larger collisional cross-section than do the atomic ions with the same mass, thus they collide more frequently and lose more energy than the analyte ions, such that they can be selectively denied entrance into the MS section *via* a decelerating potential.<sup>16,17</sup> However, for this process to be efficient, conditions are such that also a large fraction of analyte ions are removed, and thus, this compromises sensitivity. Therefore, especially for challenging situations, the use of a reactive gas (*e.g.*, H<sub>2</sub>, NH<sub>3</sub> or O<sub>2</sub>) is usually preferred, although also their use is not always self-evident. With chemical resolution based on selective ion–molecule reactions, spectral overlap from both atomic and molecular interfering ions with the same  $m/z$  as that of the corresponding analyte ion can be addressed.<sup>18</sup> The gas reacts either with the interfering ions, enabling the target element to be measured at the original  $m/z$  (on-mass), or with the analyte ion, resulting in a new reaction product ion that can be measured interference-free at another  $m/z$  (mass-shift). Selection of the best suited reaction gas is crucial, whereby it has to be taken into account that the more reactive the gas, the higher the efficiency of the reaction and thus, the expected sensitivity, but also the higher the possibility of creation of new spectral interferences, arising from ions that are formed *via* reactions between the reaction gas and concomitant matrix elements.<sup>19</sup> For conventional ICP-CRC-QMS instruments, the relatively poor control over the reaction cell chemistry in the context of mass-shift approaches has usually limited applications to gases giving rise to predictable reaction product ions and/or for on-mass approaches. In other words, for the most demanding applications, the potential of ICP-CRC-QMS instruments has been trimmed down by the lack of control of the cell chemistry when using highly reactive gases.



*Martín Resano (Ph.D. 1999, University of Zaragoza). After a post-doctoral period at Ghent University (Belgium), he became Professor of Analytical Chemistry at the University of Zaragoza in 2003. He currently leads the research group M.A.R.T.E. and devotes his research to the investigation of the capabilities of atomic spectrometry techniques for bulk and spatially resolved trace and*

*isotopic analysis of solid samples, complex clinical samples, and for the characterization of metallic NPs, topics to which he has contributed with more than 100 publications. He has been associated with JAAS Boards since 2009, and currently chairs the JAAS Editorial Board.*



*Frank Vanhaecke is Senior Full Professor at the Department of Analytical Chemistry of Ghent University (Belgium), where he leads the 'Atomic & Mass Spectrometry – A&MS' research group. His research group focuses on the determination, speciation and isotopic analysis of (trace) elements using ICP-mass spectrometry (ICP-MS). The A&MS group studies fundamentally-oriented aspects*

*of the technique and develops methods for solving challenging scientific problems in an interdisciplinary context. Frank is (co) author of ~350 journal papers. He was the chairman of the editorial board of JAAS from June 2012–June 2016 and is now member of its International Advisory Board.*

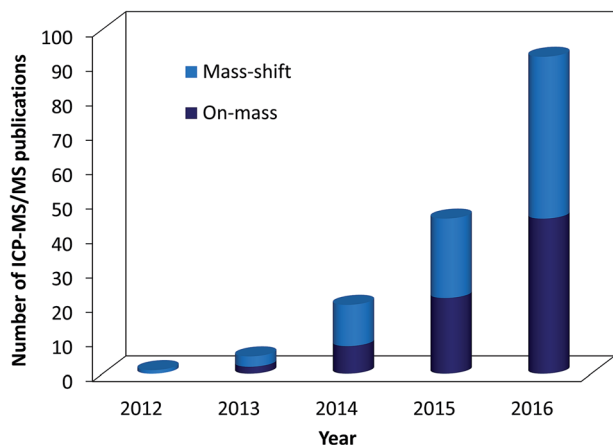


Fig. 1 Number of journal publications reporting on the use of on-mass and mass-shift ICP-MS/MS approaches.

In 2012, the introduction of a new type of quadrupole-based ICP-MS device (ICP-tandem mass spectrometer) has improved the control over the cell chemistry and has brought the concept of chemical resolution as a means to avoid spectral overlap to a higher level. In 2015 (3 years after its commercial introduction), Balcaen *et al.*<sup>20</sup> reviewed the capabilities of ICP-MS/MS for achieving interference-free conditions for elemental and isotopic analysis of elements suffering from strong spectral overlap and provided examples of real-life applications reported by early adopters of the novel technique. In a general review on spectral interference by ICP-MS by Lum *et al.*<sup>21</sup> ICP-MS/MS was also recognized as one of the most powerful strategies in this context. Since its introduction, the use of ICP-MS/MS has grown very fast, as indicated by the number of scientific publications on the topic published over the years (Fig. 1). This tutorial review aims to describe the particularities of ICP-MS/MS instrumentation, the different modes of operation and the scanning options as key tools for method development for interference-free ultra-trace element determination and to provide an overview of the most demanding recent applications reported on in the literature.

## 2. ICP-tandem mass spectrometry (ICP-MS/MS)

### 2.1. Instrument set-up

The only ICP-tandem mass spectrometers currently available on the market are the Agilent 8800 (2012) and 8900 (2016). These instruments are often referred to as triple quadrupole ICP-MS or ICP-QQQ units (Agilent Technologies – Fig. 2). Therefore, for the description of the instrumental set-up, this specific instrumentation needs to be referred to.

An ICP-tandem mass spectrometer can be seen as a conventional ICP-CRC-QMS unit with an additional quadrupole located before the CRC (Q1-CRC-Q2). This configuration (MS/MS) provides an improved control over the cell chemistry, as in MS/MS mode, *i.e.* with both quadrupoles acting as a mass filter with an approx. 1 amu bandpass window, only ions of a given  $m/z$  – analyte ion and interfering ion(s) – are allowed to enter the CRC. Next to the possibility to use the previously mentioned collision and reaction gases, this improved control over the processes taking place in the CRC also simplifies the use of non-conventional, more reactive gases, that typically produce many different reaction product ions owing to their high reactivity or more complex reaction behavior (*e.g.*, CH<sub>3</sub>F and NH<sub>3</sub>), thus providing the user with additional means to deal with spectral overlap.

ICP-MS/MS is a versatile technique, and next to the double mass selection approach (MS/MS) outlined before, the mass window of the first quadrupole can be adapted from approx. 1 amu to fully open, depending on the challenge posed by each specific application. In the rest of this review, the mode with double mass selection will be termed MS/MS mode, in contrast to that in which the first quadrupole is operated with a wider bandpass, referred to as “open”/single quadrupole or SQ mode.

Table 1 provides an overview of the different operation modes, scanning options and measurement approaches enabled by the tandem MS configuration, as described in the following sections.

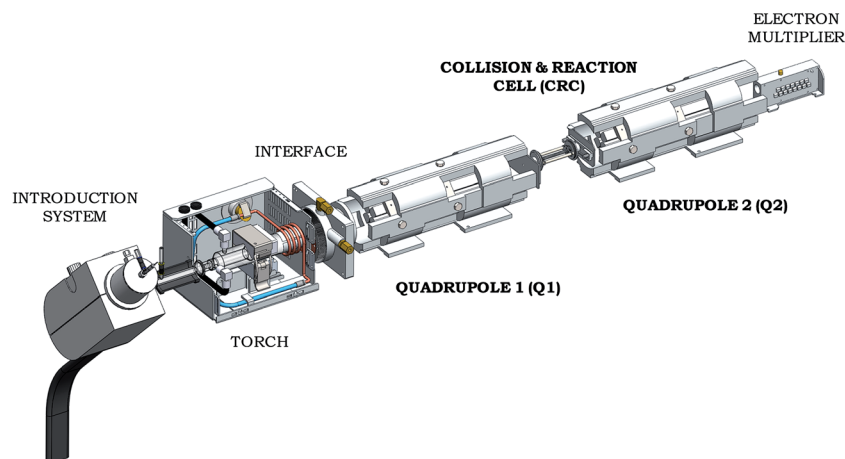


Fig. 2 Graphical representation of an ICP-tandem mass spectrometer – based on the Agilent 8800 ICP-QQQ instrument (Agilent Technologies).

Table 1 Overview of the different ICP-MS/MS operation modes enabled by the tandem MS configuration

	First quadrupole (Q1)	Second quadrupole (Q2)
SQ mode	Fully open (ion guide)	Fixed $m/z$ ratio
MS/MS mode	Fixed $m/z$ ratio	Fixed $m/z$ ratio
On-mass approach	$m/z$ Q1	$m/z$ Q2 = $m/z$ Q1
Mass-shift approach	$m/z$ Q1	$m/z$ Q2 $\neq$ $m/z$ Q1
Product ion scan	Fixed $m/z$ ratio	Scan (2–260 amu)
Precursor ion scan	Scan (2–260 amu)	Fixed $m/z$ ratio
Neutral gain scan	Scan (2–260 amu) $m/z$ Q1	Scan (2–260 amu) $m/z$ Q2 = $m/z$ Q1 + $\Delta m/z^a$

<sup>a</sup>  $\Delta m/z$  is constant over the entire mass spectrum (2–260 amu).

## 2.2. Operation modes: SQ vs. MS/MS

The ICP-tandem mass spectrometer instrument can be used in either SQ or MS/MS mode. When the instrument is working in SQ mode (Fig. 3A), Q1 can be operated as an ion guide only or as a bandpass mass filter. In the first case, Q1 is “fully open”, thus all ions – the analyte ( $^{m_1}A^+$ ) ion and the interfering ions with the same  $m/z$  ( $^{m_1}I^+$ ), but also other concomitant ions with different  $m/z$  ( $^{m_2}C^+$ ) enter the CRC. This approach resembles the situation with a conventional ICP-CRC-QMS device and can be used in the case of less demanding applications, without the presence of interfering ions or in the case of simple matrices. By means of an appropriate selection of instrumental parameters, Q1 can also be used as a bandpass mass filter, thus only allowing those ions within a specific  $m/z$  range to reach the CRC. The bandpass mode resembles an ICP-QMS instrument equipped with a quadrupole-based CRC, typically termed dynamic reaction cell (ICP-DRC-QMS). However, the true benefit of an ICP-tandem mass spectrometer is provided by the possibility of using double mass selection in the MS/MS mode (Fig. 3B), although it needs to be pointed out that the use of this mode leads to

a reduction in ion transmission efficiency, and thus sensitivity, in comparison to the SQ mode. In this approach, both Q1 and Q2 act as a real mass filter (1 amu bandpass), with both quadrupoles selecting the same  $m/z$  in the on-mass approach or different  $m/z$ 's in the mass-shift approach, depending on whether, respectively, the interfering or the analyte ion reacts with the reaction gas added. In this MS/MS mode, a specific  $m/z$  (that of the target ion –  $^{m_1}A$ ) is selected in Q1, such that only the analyte ion and the interfering ions with the same  $m/z$  ( $^{m_1}I^+$ ) are able to enter the CRC. All concomitant ions with different  $m/z$  ( $^{m_2}C^+$ ) are efficiently removed by Q1, which brings important advantages, *i.e.* (i) avoidance of unwanted product ions resulting from reactions between other ions and the reaction gas, (ii) a reduction of non-spectral interferences or matrix effects, affecting the reactions proceeding in the cell, and (iii) an improvement in efficiency of the ion–molecule chemistry occurring in the cell. These advantages result in higher capabilities for interference-free ultra-trace element determination and isotopic analysis, as enabled by using different reaction gases and adequate selection of the best reaction product ion to be monitored. Of course, this selection is not always self-evident, but some systematic methodologies can be relied on in order to find the best approach, leading to highest sensitivity and lowest detection limit. The next section provides information on the use of different scanning options in the context of method development in ICP-MS/MS.

## 2.3. Scanning options

In tandem mass spectrometry, the use of specific scanning options enables monitoring and identification of precursor and/or product ions. These scanning options can be seen as powerful tools providing an enhanced insight into the potentially complex reactions taking place in the cell and thus, they facilitate the development of interference-free measurement methodologies. In this context, the MS/MS configuration of an ICP-tandem mass spectrometer enables using product ion, precursor ion and neutral mass gain/loss scans.

**2.3.1. Product ion scan.** In ICP-MS/MS, the product ion scan is used for identification of the best suited reaction product ion formed upon reaction between the original analyte ion and the reaction gas within the cell, aiming at obtaining interference-free conditions with the highest signal-to-background ratio. In order to perform a product ion scan (see Fig. 4A), Q1 should be fixed at a specific nominal  $m/z$ , typically

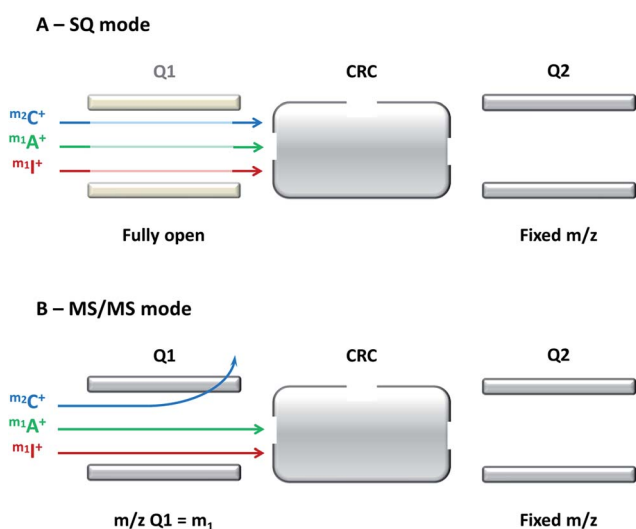


Fig. 3 Schematic representation of both operation modes – SQ (A) and MS/MS (B) – in ICP-tandem mass spectrometry.  $A^+$ ,  $C^+$  and  $I^+$  represent the analyte ion, the concomitant matrix ions with different  $m/z$  and the interfering ions with the same  $m/z$  as the analyte, respectively.

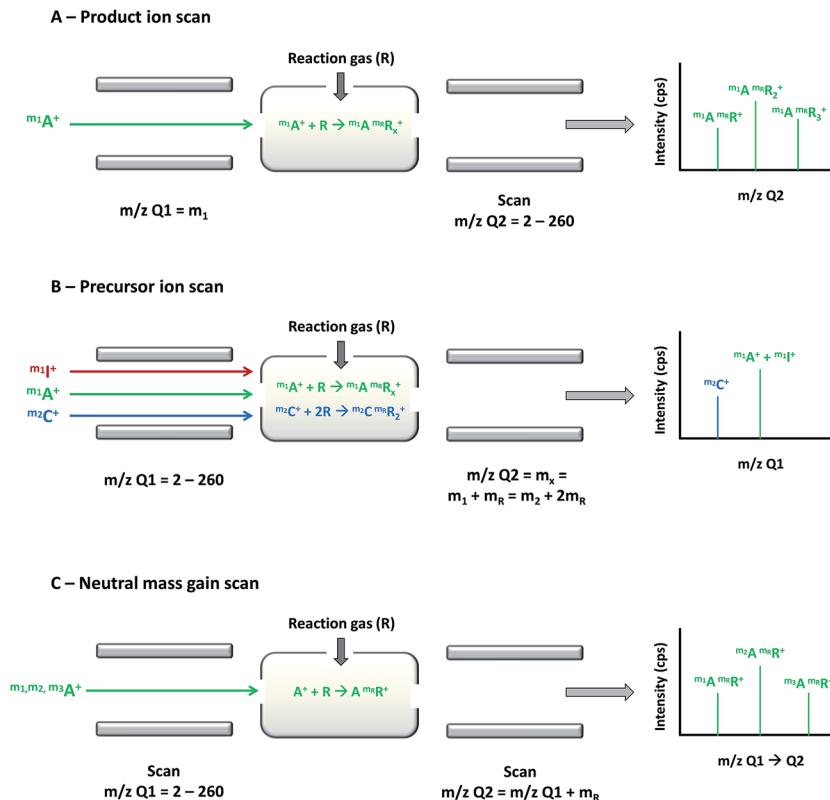


Fig. 4 Schematic representation of the operating principles for the different scanning options available in ICP-MS/MS. (A–C) correspond to product ion scan, precursor ion scan and neutral mass gain scan, respectively.  $A^+$ ,  $C^+$  and  $I^+$  represent the analyte ion, the concomitant matrix ions with different  $m/z$  and the interfering ions with the same  $m/z$  as the analyte, respectively.

that of the most abundant analyte ion ( $m_1 A$ ), although it can also be used to evaluate the effect of a specific reaction gas on a potentially interfering ion. With the  $m/z$  of Q1 fixed at  $m_1$  and the cell pressurized with the reaction gas (R), leading to different reaction product ions (e.g.,  $m_1 A^m R_x^+$ ), all product ions formed can be revealed by scanning Q2, thus covering the entire mass range (from 2 to 260 amu). From the product ion spectrum thus obtained, the reaction product ion best suited can be selected for subsequent method development.

**2.3.2. Precursor ion scan.** As opposed to a product ion scan, a precursor ion scan (see Fig. 4B) is performed to obtain more insight into the origin of a specific product ion, resulting from a reaction between a so far unidentified ion and the reaction gas (R) within the cell, which might hinder interference-free determination of the analyte ion or a reaction product ion thereof. *Via* precursor ion scanning, the  $m/z$  of the product ion selected is fixed by Q2, and with the cell pressurized with the reaction gas, a precursor ion spectrum is obtained upon scanning the entire mass range (2–260 amu) with Q1. From the spectrum thus obtained, precursor ions giving rise to spectral overlap at the  $m/z$  of interest can be identified, which might elucidate the origin of inaccurate results, resulting from a contribution of unexpected product ions to the signal intensity measured for the target analyte, if the system would be operated in SQ mode.

**2.3.3. Neutral mass gain/loss scan.** Tandem mass spectrometry also allows neutral mass gain/loss scanning, in which both quadrupoles are used in scanning mode with a fixed difference in  $m/z$  between them, instead of keeping Q1 or Q2 fixed at a specific  $m/z$ . Both gain or loss of mass can be looked for, depending on whether the precursor ion is lower or higher in mass than the corresponding product ion. In molecular tandem mass spectrometry, where a precursor ion is fragmented by collision-induced dissociation (CID), a neutral mass loss scan can be performed, e.g., to reveal which molecular ions lose a neutral fragment of given mass (e.g.,  $H_2O$ ) upon collision. However, in ICP-MS/MS, neutral mass gain scan is typically of greater interest, as the precursor ions will most often be lighter. Such a neutral mass gain scan can be accomplished by synchronous scanning of Q1 and Q2, thereby maintaining a constant difference in  $m/z$  between both. This constant ( $K = m/z(Q2) - m/z(Q1)$ ) has a value  $>0$  in neutral mass gain scan and a negative one in neutral mass loss scan ( $K < 0$ ). The main goal of a neutral gain scan (see Fig. 4C) for ICP-MS is the study of the isotopic pattern of a target element of interest (A). As a general example, we assume an element with three isotopes ( $m_1, m_2, m_3 A$ ) and a reactive gas (R), reacting with the original analyte ions as follows:  $m_1, m_2, m_3 A^+ + m_R R \rightarrow m_1, m_2, m_3 A^m R^+$ . The neutral gain scan can be used to evaluate if the set of reaction product ions  $m_1, m_2, m_3 A^m R^+$  shows the same isotopic pattern as does the set of

corresponding precursor ions. Thus, Q1 is selected at  $m/z = m_1$ ,  $m_2$  and  $m_3$  and Q2 at  $m/z = m_1 + m_R$ ,  $m_2 + m_R$  and  $m_3 + m_R$ , respectively, so that  $K = m_R$  during the entire scanning process. The neutral mass gain spectrum obtained in this way is a valuable tool for method development, especially in the context of isotopic analysis.

#### 2.4. Abundance sensitivity

ICP-MS/MS also provides an improved abundance sensitivity (AS). By definition, AS is calculated as the ratio of the maximum ion current recorded at a specified  $m/z$  value to the maximum ion current arising from the same species recorded at a neighboring  $m/z$  value ( $m/z - 1$  or  $m/z + 1$ ). Thus, it is a measurement of the contribution of the peak tail of a spectral peak (with a certain  $m/z$  value) to the signal intensity at an adjacent  $m/z$  value. This value is dependent on the resolving power of the mass spectrometer.<sup>22</sup> For a quadrupole mass spectrometer (QMS), the AS is in the order of  $\sim 10^7$ , which means that for a signal of  $10^7$  counts, at a specific  $m/z$ , there is a contribution of 1 count to the neighboring signals (at  $m/z - 1$  and  $m/z + 1$ ). An increase in AS was shown when operating the QMS at higher stability regions.<sup>23</sup> Additionally, the introduction of a non-reactive collision gas (e.g., He) in the CRC might lead to a slight improvement of the AS ( $10^8$ ), although this is accompanied by a significant drop in sensitivity.<sup>24</sup> This improvement is a result of the reduction in the spread of the kinetic energy of the atomic ions.<sup>25</sup> While the contribution of a spectral peak to the intensity at neighboring  $m/z$  values, or even  $m/z$  values that are even further away, is very small, it can become meaningful in the determination of ultra-trace amounts of an analyte element in a matrix containing very high amounts of the adjacent element, or in the determination of extreme isotope ratios, whereby the nuclides considered show a pronounced difference in abundance, (e.g.,  $^{234}\text{U}/^{238}\text{U}$  or  $^{236}\text{U}/^{238}\text{U}$ ). For an ICP-tandem mass spectrometer operated in MS/MS mode, both quadrupoles have an AS of  $\sim 10^7$ , making the overall AS to be the product of the AS for Q1 multiplied by that for Q2 ( $\text{AS}_{\text{ICP-MS/MS}} = \text{AS}_{\text{Q1}} \times \text{AS}_{\text{Q2}}$ ). This leads to a theoretical AS of  $\sim 10^{14}$ , which suffices for the most demanding applications, and adds an additional benefit to ICP-MS/MS. However, because of the narrower dynamic range of the detector this type of instrumentation is equipped with, it cannot be experimentally evaluated if an AS of  $10^{14}$  is genuinely obtained, but the AS for ICP-MS/MS is shown to be at least  $\sim 10^{10}$ .

#### 2.5. Overcoming spectral overlap: on-mass and mass-shift approaches

Before starting with the description of some applications based on the use of ICP-MS/MS, and although the concepts of on-mass and mass-shift approaches as a means to overcome spectral overlap have been addressed very briefly in the previous sections already, it is worthwhile to describe both approaches in more detail. The difference between both lies in the strategy selected to circumvent the problem of spectral interference. For the on-mass approach (sometimes also called direct determination), both Q1 and Q2 are set at the same  $m/z$ , i.e. that of the

original analyte ion of interest ( $^{m_1}\text{A}$ ). The reaction between the reaction gas (R) and the interfering ion(s) ( $^{m_1}\text{I}^+$ ) is counted on for completely removing the contribution of this (these) ion(s) to the signal intensity measured at this  $m/z$ . The newly formed reaction product ion(s) ( $^{m_1}\text{I}^{m_R}\text{R}^+$ ) is (are) removed by means of Q2, while the analyte ion of interest is measured at its original  $m/z$ . This approach is also often relied on in conventional ICP-CRC-QMS, although it needs to be pointed out that enhanced control over the reaction cell chemistry is obtained in ICP-MS/MS due to the capability of Q1 to reject all concomitant ions with an  $m/z$  different from that of the analyte ion ( $^{m_R}\text{C}^+$ ). In this way, the formation of new, unwanted reaction product ions with the same  $m/z$  as that of the analyte ion and thus interfering with its determination can be avoided (Fig. 5A). It is clear that the on-mass approaches have been further perfected with the introduction of ICP-MS/MS, however, quantitative conversion of the interfering ion into another species is mandatory. This requisite is particularly important if the interfering ion is present at much higher levels than the analyte, such that even a small portion of it not reacting can significantly affect the results. Unfortunately, this requisite is not always fulfilled.

In traditional ICP-CRC-QMS, the mass-shift approach (sometimes called indirect determination) is often hampered by the lack of control over the ion-molecule chemistry proceeding in the reaction cell. The introduction of ICP-MS/MS now allows

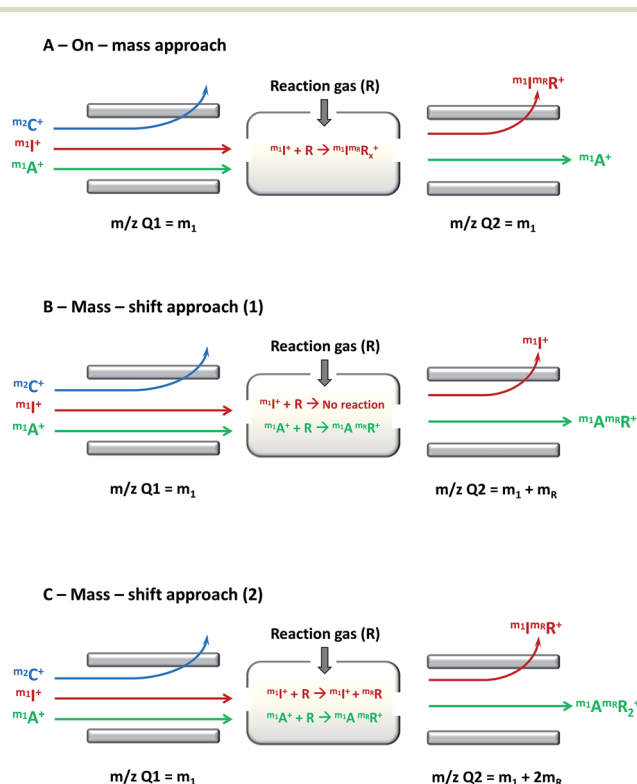


Fig. 5 Schematic representation of the different approaches, on-mass (A) and mass-shift (B and C) used to overcome spectral overlap in ICP-MS/MS. Mass-shift approaches rely either on the absence of reaction for the interfering ion ( $^{m_1}\text{I}^+$ ) towards the reaction gas (R) – B, or a different reaction behavior between analyte ( $^{m_1}\text{A}^+$ ) and interfering ion ( $^{m_1}\text{I}^+$ ) towards R – C.

one to fully exploit the capabilities of reaction gases as well. For such a mass-shift approach, Q1 is fixed at the original  $m/z$  of the analyte ion of interest ( ${}^{m_1}\text{A}^+$ ), such that only interfering ions with the same  $m/z$  ( ${}^{m_1}\text{I}^+$ ) are also able to reach the CRC, while all other ions with different  $m/z$ 's ( ${}^{m_2}\text{C}^+$ ) are removed. The CRC is pressurized with a reaction gas, which has to show a high reactivity towards the analyte ion and no reactivity (Fig. 5B) or a different behavior (Fig. 5C) towards the interfering ion(s). In case several types of reaction product ions are formed, the best suited reaction is selected and the Q2 is fixed at the corresponding  $m/z$ . Ions that interfere with the determination of the analyte ion at its original  $m/z$  will enter the cell, but they are rejected by Q2 when they show no (or

a different) reactivity towards the reaction gas. It has to be mentioned that although a high conversion efficiency for the analyte ion is advantageous, quantitative conversion is not mandatory. Therefore, mass-shift seems to provide more versatility to avoid spectral overlap, and that is why this strategy is typically preferred over the on-mass approach for obtaining interference-free conditions for elemental and isotopic analysis. Fig. 6 provides an overview guiding the user to the ICP-MS/MS strategy best suited for addressing the specific application at hand, characterized by, among other, the type of spectral interference, the analyte concentration and/or the matrix composition.

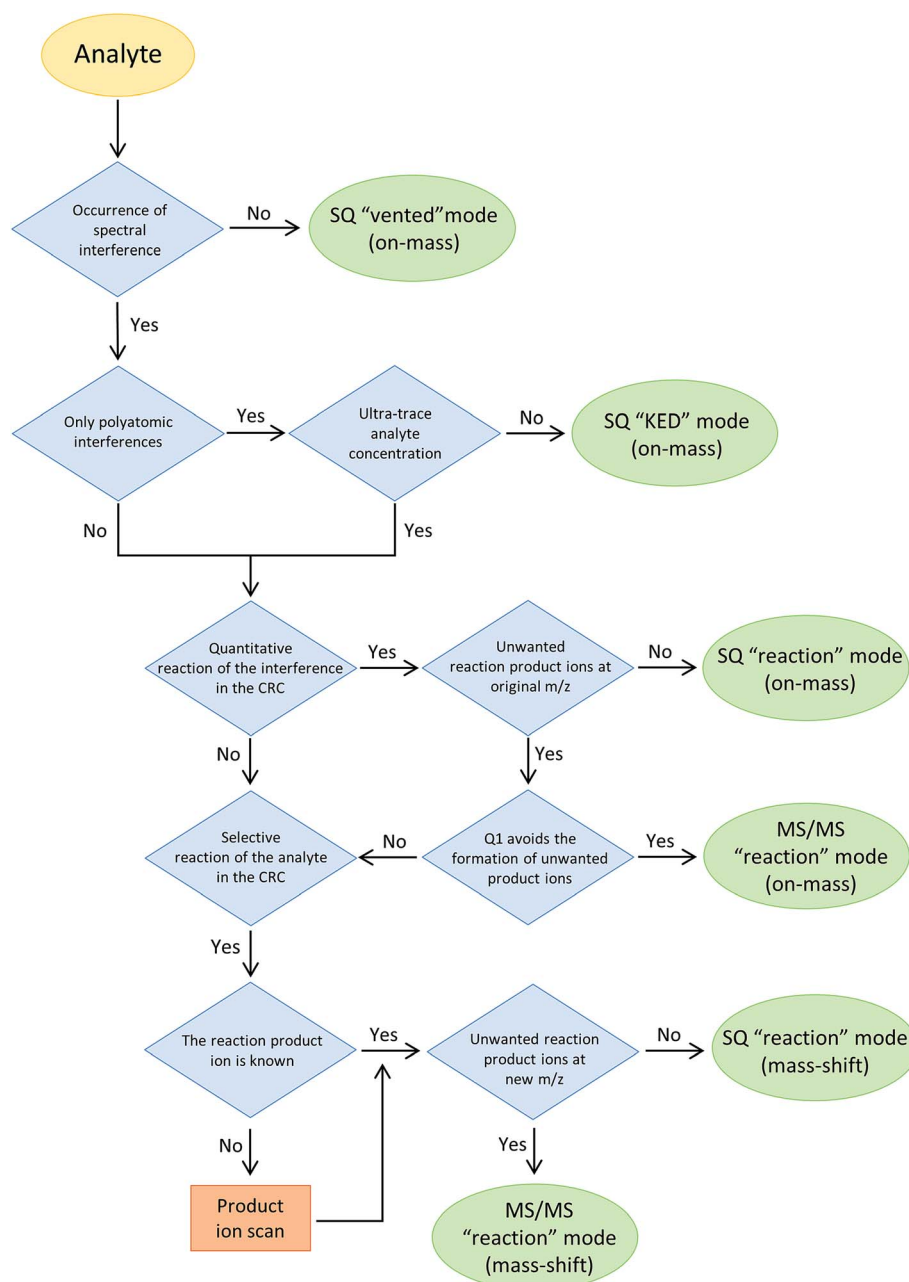


Fig. 6 Flow chart indicating the user to a suitable approach to avoid spectral overlap using ICP-MS/MS.

### 3. Applications

As stated above, ICP-MS/MS has only been introduced recently. Nevertheless, several approaches reported on in the literature have already demonstrated the added value of this novel set-up. In this section, some of the applications described in the literature are summarized with the focus on the improvements obtained owing to the use of ICP-MS/MS, and paying attention to the different approaches and tools for method development, as described in preceding sections. Next to quantitative elemental analysis, also applications in the field of isotopic analysis have been selected, as well as examples of hyphenated set-ups, where an ICP-tandem mass spectrometer is used in combination with different introduction systems, including separation techniques (see Table 2 for a list of papers reporting on ICP-MS/MS).

#### 3.1. Elemental analysis

**3.1.1. Mono-elemental analysis.** Owing to the enhanced control over the reaction chemistry taking place in the reaction cell, the applicability of the mass-shift approach for dealing with spectral interferences has largely increased with the introduction of ICP-MS/MS. Oxygen ( $O_2$ ) is one of the most frequently used reaction gases in ICP-CRC-QMS and its use has been widely described in the literature. Many elements show reactivity towards  $O_2$ , with O-atom transfer being the most common ion-molecule reaction. Thus, a target ion ( $A^+$ ) is converted into a reaction product ion ( $AO^+$ ) with a gain in  $m/z = 16$ . This reaction can be used both for on-mass and mass-shift approaches depending on whether the reaction takes place with the interfering or the analyte ion, respectively. The applicability of  $O_2$  (as well as of other reaction gases) in conventional ICP-QMS or in ICP-MS/MS operated in SQ mode, might be limited by the formation of unwanted reaction product ions with the same  $m/z$  as that of the target analyte or the corresponding reaction product ion and/or by the presence of concomitant elements with the same  $m/z$  as that of the reaction product ion selected (in mass-shift approaches). In this context, the addition of an extra quadrupole in the ICP-tandem mass spectrometer operating in MS/MS mode has been successfully used to overcome the spectral overlap. Virgilio *et al.*<sup>26</sup> studied the reactivity and performance of  $O_2$  as reaction gas in ICP-MS/MS for a list of selected analytes with different affinity towards  $O_2$ . This work is intended to be used as a guide for selecting the best approach aiming to overcome the spectral interferences by means of on-mass and mass-shift (+16 amu and/or +32 amu) approaches using  $O_2$  in MS/MS mode. In addition, these approaches have already been used in very diverse and challenging applications. For instance, it is well known that the determination of arsenic ( $^{75}As$ ) is hampered by the occurrence of both non-spectral<sup>27</sup> and spectral interferences<sup>28</sup> (caused by the occurrence of, e.g.,  $^{40}Ar^{35}Cl^+$ ,  $^{38}Ar^{37}Cl^+$ ,  $^{40}Ca^{35}Cl^+$  and/or  $^{59}Co^{16}O^+$  polyatomic ions, and of  $^{150}Nd^{2+}$  and  $^{150}Sm^{2+}$  doubly charged ions). By using  $O_2$  as a reaction gas in ICP-MS/MS,  $^{75}As^+$  ions are converted into the corresponding  $^{75}As^{16}O^+$  reaction product ions ( $m/z = 91$ ). While in SQ mode, the presence of  $^{59}Co$

( $^{59}Co^+ + O_2 \rightarrow ^{59}CoO^+$ ,  $^{59}CoO^+ + O_2 \rightarrow ^{59}CoO_2^+$ ;  $m/z = 91$ ) and  $^{91}Zr$  hinder the indirect measurement of  $^{75}As^+$  as  $^{75}AsO^+$ , the use of Q1 in the MS/MS mode allows for an interference-free determination by removing all ions with  $m/z \neq 75$  (except when a significant amount of  $CoO^+$  is formed already in the plasma as the result of a very high concentration of Co in the sample matrix). Another example is the work of Meyer *et al.*,<sup>29,30</sup> in which As was determined as the corresponding  $AsO^+$  reaction product ion for the characterization of As-containing hydrocarbons (AsHCs), with the aim of evaluating the toxicity of these species during *in vitro* and *in vivo* studies.

Sulphur (S) is another element that suffers from strong spectral overlap, mainly from O-based polyatomic interferences. The reaction with  $O_2$  leads to the formation of  $SO^+$  product ions. However, as indicated in Table 3,<sup>31</sup>  $SO^+$  reaction product ions are not free from spectral interference, which limits the applicability of this approach for single quadrupole ICP-(CRC-)QMS systems. However, ICP-MS/MS operated in MS/MS mode enables interference-free measurement of  $S^+$  as  $SO^+$  owing to the capability of Q1 to efficiently get rid of ions with  $m/z \neq 32$ , 33 and 34, respectively. In this way, only those ions with  $m/z = 32$ , 33 and 34, respectively, can reach the cell and react with  $O_2$ . The determination of S *via* reaction with  $O_2$  in a mass-shift approach using ICP-MS/MS can be seen as one of the leading applications due to the relevance of S in many different contexts. For instance, a mono-element method for the direct quantification of sulfur dioxide ( $SO_2$ ) in wine (food safety) was developed by Wang *et al.*<sup>32</sup> The method developed was also successfully used for the quantification of other S-containing compounds. Other applications in which the determination of S is of high interest are described in the next sections.

The determination of trace amounts of selenium (Se) can also be accomplished in MS/MS mode with  $O_2$  mass-shift approaches. The signals of the Se isotopes are affected by, among other, Ar-based polyatomic ions, Ar dimers being the most problematic ones. In this case, even the maximum resolution attained by present-day commercially available high resolution SF-ICP-MS instrumentation is not able to resolve the spectral overlap of the signals of  $^{40}Ar_2^+$  and  $^{80}Se^+$ , the most abundant Se isotope (49.6%). The conversion of  $Se^+$  ions into the corresponding  $SeO^+$  product ions in an ICP-tandem mass spectrometer allows for an interference-free determination by removing both polyatomic and doubly charged ( $Gd^{2+}$ ) interfering ions. In the work of Bishop *et al.*,<sup>33</sup> Se was determined in the presence of a high concentration of Gd in serum samples, simulating the result of a Gd-based magnetic resonance imaging (MRI). A schematic diagram explaining the operating principles of MS/MS for the interference-free determination of Se using an on-mass ( $H_2$ ) and mass-shift approach ( $O_2$ ) is provided as Fig. 7 (Sugiyama *et al.*<sup>34</sup>).

Next to O-atom transfer, another option to avoid spectral overlap with  $O_2$  is the charge transfer reaction. The reaction mechanism involves the conversion of analyte or interfering ions into the corresponding neutral species, while  $O_2$  is converted into the  $O_2^+$  ion ( $m/z = 32$ ). This reaction can be used to avoid spectral overlap by neutralizing interfering ions, and measuring the analyte ion at its original  $m/z$  (on-mass

Table 2 Compilation of ICP-MS/MS works reported on in literature

Analyte ion (nuclide mass)	Potential interfering ion(s) <sup>a</sup>	Reaction gas (mL min <sup>-1</sup> )	Measured ion	LoDs <sup>b</sup>	Additional information
Ag <sup>+</sup> (107, 109)	ArZn <sup>+</sup> , NbO <sup>+</sup> , YO <sup>+</sup> , ZrO <sup>+</sup>	NH <sub>3</sub> (7)	Ag <sup>+</sup>	0.8–1.5 pg g <sup>-1</sup>	Matrix solutions (1 µg g <sup>-1</sup> Nb, Y, Zn, Zr) <sup>34*</sup>
Al <sup>+</sup> (27)	CN <sup>+</sup> , HCN <sup>+</sup>	O <sub>2</sub> (0.5) CH <sub>3</sub> F (1)	Al <sup>+</sup> AlCH <sub>3</sub> F <sup>+</sup>	200 ng L <sup>-1</sup> 8 ng L <sup>-1</sup>	HNO <sub>3</sub> (1% v/v) <sup>26*</sup> Biofluids <sup>47*,48*</sup>
As <sup>+</sup> (75)	ArCl <sup>+</sup> , Ar <sub>2</sub> H <sup>+</sup> , ArK <sup>+</sup> , CaO <sub>2</sub> <sup>+</sup> , CoO <sup>+</sup>	He (3) O <sub>2</sub> (0.1–0.7)	As <sup>+</sup> AsO <sup>+</sup>	N.A. 1–13 ng L <sup>-1</sup> ; 0.0015–24 ng g <sup>-1</sup> ; 0.3 ng per unit	HPLC-ICP-MS/MS: seafood <sup>73*</sup> HNO <sub>3</sub> (1% v/v) <sup>26*</sup> , hydrocarbons, <sup>29,30</sup> food and beverages <sup>42*,74*,75</sup> , arsenolipids; <sup>76</sup> food <sup>77*</sup> , tobacco <sup>78*</sup> , crude oils <sup>79*</sup> ; cigarette smoke <sup>80*</sup>
Au <sup>+</sup> (197)	ArGd <sup>+</sup> , HfO <sup>+</sup> , HfOH <sup>+</sup> , TaO <sup>+</sup> <sup>12</sup> C <sup>+</sup> tail	CH <sub>3</sub> F (0.7) NH <sub>3</sub> (4)	AsCH <sub>2</sub> <sup>+</sup> Au(NH <sub>3</sub> ) <sub>2</sub> <sup>+</sup>	0.2 ng L <sup>-1</sup> 1 pg g <sup>-1</sup>	HPLC-ICP-MS/MS: urine, <sup>63,64</sup> human cells, <sup>81</sup> fish oil; <sup>82</sup> brain astrocytes <sup>83</sup> HG-ICP-MS/MS: rice and samples of marine origin <sup>65,84</sup> Environmental samples <sup>41</sup> Matrix solution (10 µg g <sup>-1</sup> Gd, Hf, Ta) <sup>34*</sup>
B <sup>+</sup> (11)		O <sub>2</sub> (0.3)	B <sup>+</sup>	0.4 µmol B mol <sup>-1</sup> Ca	Carbonates <sup>43*</sup>
Ba <sup>+</sup> (138)	Ce <sup>+</sup> , La <sup>+</sup> , SnO <sup>+</sup> , TeO <sup>+</sup>	O <sub>2</sub> (0.1)	Ba <sup>+</sup>	5 ng L <sup>-1</sup>	HNO <sub>3</sub> (1% v/v) <sup>26*</sup>
Bi <sup>+</sup> (209)	IrO <sup>+</sup>	O <sub>2</sub> (0.1)	Bi <sup>+</sup>	2 ng L <sup>-1</sup>	HNO <sub>3</sub> (1% v/v) <sup>26*</sup>
Br <sup>+</sup> (79)	Ar <sub>2</sub> H <sup>+</sup> , ArK <sup>+</sup> , PO <sup>+</sup>	H <sub>2</sub> (3)	Br <sup>+</sup>	0.4 µg L <sup>-1</sup>	HPLC-ICP-MS/MS: blood plasma <sup>61*</sup>
C <sup>+</sup> (12)	Mg <sup>++</sup>	O <sub>2</sub> (0.7)	CO <sup>+</sup>	0.2 mg L <sup>-1</sup>	Aminoacids <sup>85*</sup>
Ca <sup>+</sup> (40, 42, 46)	Ar <sup>+</sup> , ArH <sub>2</sub> <sup>+</sup> , NO <sub>2</sub> <sup>+</sup> , SN <sup>+</sup>	O <sub>2</sub> (0.3) SF <sub>6</sub> /H <sub>2</sub> (0.03/5)	Ca <sup>+</sup> CaF <sup>+</sup>	N.A.	Carbonates <sup>43*</sup>
Cd <sup>+</sup> (110, 111, 112, 113, 114)	Ar <sub>2</sub> O <sub>2</sub> <sup>+</sup> , Ca <sub>2</sub> O <sub>2</sub> <sup>+</sup> , MoO <sup>+</sup> , RuO <sup>+</sup> , Sn <sup>+</sup> , ZrO <sup>+</sup>	O <sub>2</sub> (0.3–0.6)	Cd <sup>+</sup>	4–16 ng L <sup>-1</sup> ; 2 ng g <sup>-1</sup> ; 1 ng per unit 11 nmol QDs L <sup>-1</sup> , 0.2 ng L <sup>-1</sup> (0.2 fmol))	Minerals (isotopic analysis) <sup>86</sup> Milk <sup>44*</sup> , tobacco <sup>78*</sup> ; sediments, fertilizer and sludge <sup>45*</sup> ; cigarette smoke <sup>80*</sup> FFF-ICP-MS/MS: quantum dots <sup>67,68,87</sup>
Ce <sup>+</sup> (140, 141)	BaH <sup>+</sup> , SbO <sup>+</sup> , SnO <sup>+</sup> , TeO <sup>+</sup>	O <sub>2</sub> (0.1; 0.4)	CeO <sup>+</sup>	0.1 ng L <sup>-1</sup> ; 10 pg g <sup>-1</sup>	HNO <sub>3</sub> (1% v/v) <sup>26*</sup> ; quartz-rich geological samples <sup>88*</sup>
Cl <sup>+</sup> (35, 37)	ArH <sup>+</sup> , O <sub>2</sub> H <sup>+</sup> , SH <sup>+</sup>	H <sub>2</sub> (2–7)	ClH <sub>2</sub> <sup>+</sup>	1 µg L <sup>-1</sup> 0.15–0.5 µg L <sup>-1</sup>	HPLC-ICP-MS/MS: blood plasma <sup>61*</sup> GC-ICP-MS/MS: marine sediments (isotope dilution), <sup>89</sup> foods <sup>60</sup>
Co <sup>+</sup> (59)	ArF <sup>+</sup> , ArNa <sup>+</sup> , ArOH <sup>+</sup> , CaO <sup>+</sup> , CaOH <sup>+</sup> , MgCl <sup>+</sup>	NH <sub>3</sub> (6; 4)	Co(NH <sub>3</sub> ) <sub>2</sub> <sup>+</sup>	0.02 µg g <sup>-1</sup> ; 0.03 ng per unit	Tobacco <sup>78*</sup> ; cigarette smoke <sup>80*</sup>
Cr <sup>+</sup> (52, 53)	ArC <sup>+</sup> , ArN <sup>+</sup> , ArNH <sup>+</sup> , ArO <sup>+</sup> , ArOH <sup>+</sup> , ClN <sup>+</sup> , ClO <sup>+</sup> , ClOH <sup>+</sup> , SO <sup>+</sup>	CH <sub>3</sub> F (1) O <sub>2</sub> (0.3) NH <sub>3</sub> (3–6)	Co(CH <sub>3</sub> F) <sub>2</sub> <sup>+</sup> CrO <sup>+</sup> Cr(NH <sub>3</sub> ) <sub>2</sub> <sup>+</sup>	0.3 ng L <sup>-1</sup> 3 ng L <sup>-1</sup> 0.09 µg g <sup>-1</sup> ; 3 pg g <sup>-1</sup> ; 0.85 ng per unit	Biofluids <sup>47*,48*</sup> Drinking water <sup>42*</sup> Tobacco <sup>78*</sup> ; crude oils <sup>79*</sup> ; cigarette smoke <sup>80*</sup>
Cs <sup>+</sup> (134, 135, 137)	ArMo <sup>+</sup> , Ba <sup>+</sup> , Xe <sup>+</sup>	CH <sub>3</sub> F (1) N <sub>2</sub> O (0.4–3)	Cr(CH <sub>3</sub> F) <sub>2</sub> <sup>+</sup> Cs <sup>+</sup>	0.9–6 ng L <sup>-1</sup> 0.002–0.03 pg mL <sup>-1</sup>	Biofluids <sup>47*,48*</sup> Fukushima environmental samples (isotopic analysis) <sup>52–58</sup>
Cu <sup>+</sup> (63)	ArNa <sup>+</sup> , CaOH <sup>+</sup> , COCl <sup>+</sup> , NaCa <sup>+</sup> , PO <sub>2</sub> <sup>+</sup> , TiO <sup>+</sup>	O <sub>2</sub> (0.5)	Cu <sup>+</sup>	40 ng L <sup>-1</sup> 1 µg g <sup>-1</sup>	HNO <sub>3</sub> (1% v/v) <sup>26*</sup> LA-ICP-MS/MS: prostate cancer biopsy sample <sup>71</sup> Crude oils <sup>79*</sup>
Dy <sup>+</sup> (163)	SmO <sup>+</sup>	NH <sub>3</sub> (3)	Cu(NH <sub>3</sub> ) <sub>2</sub> <sup>+</sup>	19 pg g <sup>-1</sup>	Crude oils <sup>79*</sup>
Er <sup>+</sup> (166, 167)	EuO <sup>+</sup> , NdO <sup>+</sup> , SmO <sup>+</sup>	O <sub>2</sub> (0.4)	DyO <sup>+</sup>	8 pg g <sup>-1</sup>	Quartz-rich geological samples <sup>88*</sup>
Fe <sup>+</sup> (56)	ArNH <sup>+</sup> , ArO <sup>+</sup> , ArOH <sup>+</sup> , CaO <sup>+</sup> , ClOH <sup>+</sup>	O <sub>2</sub> (0.4) H <sub>2</sub> (3)	ErO <sup>+</sup>	5 pg g <sup>-1</sup>	Quartz-rich geological samples <sup>88*</sup>
Gd <sup>+</sup> (155, 157)	BF <sup>+</sup> , LaO <sup>+</sup> , PrO <sup>+</sup>	NH <sub>3</sub> (3) O <sub>2</sub> (0.4)	Fe <sup>+</sup>	2 µg g <sup>-1</sup>	LA-ICP-MS/MS: prostate cancer biopsy sample; <sup>71</sup> grey matter in Alzheimer's disease frontal cortex <sup>90</sup> Crude oils <sup>79*</sup>
Hg <sup>+</sup> (202)	OsO <sup>+</sup> , WO <sup>+</sup>	NH <sub>3</sub> (3) O <sub>2</sub> (0.4) He (3) O <sub>2</sub> (0.3)	Fe(NH <sub>3</sub> ) <sub>2</sub> <sup>+</sup> GdO <sup>+</sup> Hg <sup>+</sup>	270 pg g <sup>-1</sup> 5–7 pg g <sup>-1</sup> N.A.	Quartz-rich geological samples <sup>88*</sup> HPLC-ICP-MS/MS: seafood <sup>73*</sup>
I <sup>+</sup> (129, 131)	CdO <sup>+</sup> , InO <sup>+</sup> , Xe <sup>+</sup>	O <sub>2</sub> (0.9)	I <sup>+</sup>	38 ng L <sup>-1</sup>	Drinking water <sup>42*</sup> , HgSe fluorescent nanoparticles <sup>91</sup> Fukushima soil sediments (isotopic analysis) <sup>51,92</sup>
Ir <sup>+</sup> (191, 193)	EuAr <sup>+</sup> , HfO <sup>+</sup> , LuO <sup>+</sup>	NH <sub>3</sub> (1)	IrNH <sup>+</sup>	N.A.	Matrix solution (10 µg g <sup>-1</sup> Eu, Hf, Lu) <sup>34*</sup>
K <sup>+</sup> (40)	Ar <sup>+</sup> , Ca <sup>+</sup> , MgO <sup>+</sup> , Se <sup>++</sup>	SF <sub>6</sub> /H <sub>2</sub> (0.03/5)	K <sup>+</sup>	N.A.	Minerals <sup>86</sup>
La <sup>+</sup> (139)	BaH <sup>+</sup> , SbO <sup>+</sup> , TeO <sup>+</sup>	O <sub>2</sub> (0.1; 0.4)	LaO <sup>+</sup>	1 ng L <sup>-1</sup> ; 9 pg g <sup>-1</sup>	HNO <sub>3</sub> (1% v/v) <sup>26*</sup> ; quartz-rich geological samples <sup>88*</sup>
Lu <sup>+</sup> (175)	TbO <sup>+</sup>	O <sub>2</sub> (0.4)	LuO <sup>+</sup>	8 pg g <sup>-1</sup>	Quartz-rich geological samples <sup>88*</sup>
Mg <sup>+</sup> (24)	C <sub>2</sub> <sup>+</sup>	O <sub>2</sub> (0.1)	Mg <sup>+</sup>	0.2 µg L <sup>-1</sup>	HNO <sub>3</sub> (1% v/v) <sup>26*</sup>

Table 2 (Contd.)

Analyte ion (nuclide mass)	Potential interfering ion(s) <sup>a</sup>	Reaction gas (mL min <sup>-1</sup> )	Measured ion	LoDs <sup>b</sup>	Additional information
Mn <sup>+</sup> (55)	ArF <sup>+</sup> , ArN <sup>+</sup> , ArNH <sup>+</sup> , ArO <sup>+</sup> , ArOH <sup>+</sup> , ClO <sup>+</sup> , ClOH <sup>+</sup> , KO <sup>+</sup> , NaS <sup>+</sup>	H <sub>2</sub> (3)	Mn <sup>+</sup>	0.2 µg g <sup>-1</sup>	LA-ICP-MS/MS: prostate cancer biopsy sample <sup>71</sup>
		O <sub>2</sub> (0.3–0.6)	MnO <sup>+</sup>	3 µg g <sup>-1</sup> ; 3 pg g <sup>-1</sup> ; 0.2 ng per unit	Tobacco <sup>78*</sup> ; crude oils <sup>79*</sup> ; cigarette smoke <sup>80*</sup>
Mo <sup>+</sup> (98)	BrO <sup>+</sup> , K <sub>2</sub> O <sup>+</sup>	CH <sub>3</sub> F (1)	Mn(CH <sub>3</sub> F) <sup>+</sup>	1 ng L <sup>-1</sup>	Biofluids <sup>47*</sup>
Nd <sup>+</sup> (142, 143, 144)	RuO <sub>3</sub> <sup>+</sup>	O <sub>2</sub> (0.1, 0.5)	MoO <sub>2</sub> <sup>+</sup>	3 ng L <sup>-1</sup> ; 0.5 µg L <sup>-1</sup>	HNO <sub>3</sub> (1% v/v) <sup>26*</sup> ; milk <sup>44*</sup>
		O <sub>2</sub> (0.4)	NdO <sup>+</sup>	6–9 pg g <sup>-1</sup>	Quartz-rich geological samples <sup>88*</sup>
Ni <sup>+</sup> (58, 60)	ArO <sup>+</sup> , ArOH <sup>+</sup> , CaO <sup>+</sup> , CaOH <sup>+</sup> , NaCl <sup>+</sup> , Si <sub>2</sub> <sup>+</sup>	O <sub>2</sub> (0.6; 0.5)	NiO <sup>+</sup>	0.2 µg g <sup>-1</sup> ; 0.4 ng per unit	Tobacco <sup>78*</sup> ; cigarette smoke <sup>80*</sup>
		NH <sub>3</sub> (3)	Ni(NH <sub>3</sub> ) <sub>3</sub> <sup>+</sup>	40 pg g <sup>-1</sup>	Crude oils <sup>79*</sup>
Os <sup>+</sup> (188, 189)	ArNd <sup>+</sup> , ArSm <sup>+</sup> , YbO <sup>+</sup>	CH <sub>3</sub> F (1)	Ni(CH <sub>3</sub> F) <sub>2</sub> <sup>+</sup>	2 ng L <sup>-1</sup>	Biofluids <sup>47*,48*</sup>
		NH <sub>3</sub> (1)	OsNH <sup>+</sup>	2–4 pg g <sup>-1</sup>	Matrix solution (10 µg g <sup>-1</sup> Nd, Sm, Yb) <sup>34*</sup>
P <sup>+</sup> (31)	CO <sup>+</sup> , COH <sup>+</sup> , N <sub>2</sub> H <sup>+</sup> , NO <sup>+</sup> , NOH <sup>+</sup>	O <sub>2</sub> (0.1–0.7)	PO <sup>+</sup>	0.2–0.3 µg L <sup>-1</sup> ; 25 pg g <sup>-1</sup>	HNO <sub>3</sub> (1% v/v) <sup>26*</sup> ; (bio)diesel and oil <sup>93*</sup> ; carbonates; <sup>43</sup> crude oils <sup>79*</sup>
		N.A.		N.A.	LA-ICP-MS/MS: prostate cancer biopsy sample <sup>71</sup>
Pb <sup>+</sup> (204, 206, 207, 208)	PtO <sup>+</sup>	O <sub>2</sub> (0.5)	Pb <sup>+</sup>	7 fmol (species), 0.1 µg L <sup>-1</sup>	HPLC-ICP-MS/MS: proteomics <sup>62*</sup> , DNA-protein <sup>94*</sup>
				0.001–0.04 µg L <sup>-1</sup>	GC-ICP-MS/MS: foods <sup>60</sup>
Pd <sup>+</sup> (105, 106, 108)	ArCu <sup>+</sup> , Cd <sup>+</sup> , MoO <sup>+</sup> , SrO <sup>+</sup> , SrOH <sup>+</sup> , YO <sup>+</sup> , ZnCl <sup>+</sup> , ZrO <sup>+</sup>	O <sub>2</sub> (0.1; 0.3)	Pd <sup>+</sup>	7 ng L <sup>-1</sup> ; 0.08 ng per unit	HNO <sub>3</sub> (1% v/v) <sup>26*</sup> ; cigarette smoke <sup>80*</sup>
		NH <sub>3</sub> (7)	Pd <sup>+</sup>	2 ng L <sup>-1</sup> ; 10 ng g <sup>-1</sup>	HNO <sub>3</sub> (1% v/v) <sup>26*</sup> ; sediments, fertilizer and sludge <sup>45*</sup>
Pt <sup>+</sup> (195, 196, 198)	ArGd <sup>+</sup> , HfO <sup>+</sup> , Hg <sup>+</sup> , TaOH <sup>+</sup> , WO <sup>+</sup>	NH <sub>3</sub> (3)	Pd(NH <sub>3</sub> ) <sub>3</sub> <sup>+</sup>	0.3 pg g <sup>-1</sup>	Matrix solution (1 µg g <sup>-1</sup> Cu, Sr, Y, Zn) <sup>34*</sup>
		N.A.	Pt <sup>+</sup>	0.9 ng g <sup>-1</sup>	Moss samples <sup>46*</sup>
Rb <sup>+</sup> (85, 87)	ArSc <sup>+</sup> , ArTi <sup>+</sup> , Er <sup>++</sup> , GaO <sup>+</sup> , Sr <sup>+</sup> , Yb <sup>++</sup>	O <sub>2</sub> (0.3)	PtO <sup>+</sup>	N.A.	LA-ICP-MS/MS: tumor tissues <sup>95,96</sup>
		NH <sub>3</sub> (3)	Pt(NH <sub>3</sub> ) <sub>2</sub> <sup>+</sup>	15 ng g <sup>-1</sup>	Sediments, fertilizer and sludge <sup>45*</sup>
Rh <sup>+</sup> (103)	ArCu <sup>+</sup> , Pb <sup>++</sup> , RbO <sup>+</sup> , SrO <sup>+</sup> , ZnCl <sup>+</sup>	O <sub>2</sub> (0.3)	RhO <sup>+</sup>	0.1 ng g <sup>-1</sup> ; 1–4 pg g <sup>-1</sup>	Moss samples <sup>46*</sup> ; matrix solution (10 µg g <sup>-1</sup> Gd, Hf, Ta, W) <sup>34*</sup>
		NH <sub>3</sub> (4)	Rh <sup>+</sup>	N.A.	Minerals (isotopic analysis) <sup>86</sup>
Ru <sup>+</sup> (99, 101)	ArCu <sup>+</sup> , Pb <sup>++</sup> , RbO <sup>+</sup> , SrO <sup>+</sup> , ZnCl <sup>+</sup>	NH <sub>3</sub> (3)	Rh(NH <sub>3</sub> ) <sub>4</sub> <sup>+</sup>	2.5 ng g <sup>-1</sup>	Sediments, fertilizer and sludge <sup>45*</sup>
		NH <sub>3</sub> (4)	Ru <sup>+</sup>	0.1 pg g <sup>-1</sup>	Matrix solution (1 µg g <sup>-1</sup> Cu, Pb, Rb, Sr, Zn) <sup>34*</sup>
S <sup>+</sup> (32, 34)	MoH <sup>+</sup> , ArNi <sup>+</sup> , RbO <sup>+</sup> , ZnCl <sup>+</sup>	NH <sub>3</sub> (3)	Rh(NH <sub>3</sub> ) <sub>4</sub> <sup>+</sup>	0.2 ng g <sup>-1</sup>	Moss samples <sup>46*</sup>
		NH <sub>3</sub> (4)	Ru <sup>+</sup>	1.5 pg g <sup>-1</sup>	Matrix solution (1 µg g <sup>-1</sup> Mo, Ni, Rb, Zn) <sup>34*</sup>
Sc <sup>+</sup> (45)	NO <sup>+</sup> , NOH <sup>+</sup> , NOH <sub>2</sub> <sup>+</sup> , O <sub>2</sub> <sup>+</sup> , O <sub>2</sub> H <sup>+</sup> , SH <sup>+</sup>	O <sub>2</sub> (0.3–0.7)	SO <sup>+</sup>	1 ng g <sup>-1</sup> ; 0.3–340 µg L <sup>-1</sup>	Crude oils <sup>79*</sup> ; fed chickens <sup>97*</sup> ; carbonates, <sup>43</sup> wine, <sup>32</sup> aminoacids <sup>85*</sup> ; HgSe fluorescent nanoparticles, <sup>91</sup> (bio)diesel and oil <sup>93*</sup>
				3–6 µg L <sup>-1</sup> , 0.1–1 µmol L <sup>-1</sup>	Isotope dilution: biodiesel; <sup>31</sup> synthetic peptide standards, <sup>98</sup> proteins, <sup>99</sup> amino acid standards <sup>100</sup>
Se <sup>+</sup> (77, 78, 80, 82)	CO <sub>2</sub> <sup>+</sup> , CO <sub>2</sub> H <sup>+</sup> , N <sub>2</sub> OH <sup>+</sup> , SiO <sup>+</sup> , SiOH <sup>+</sup>	O <sub>2</sub> (0.1; 0.2)	ScO <sup>+</sup>	5.5 µg L <sup>-1</sup> , 11 fmol (species), 358 fmol	HPLC-ICP-MS/MS: proteomics <sup>62*</sup> , DNA-protein <sup>94*</sup> , intact proteins <sup>101</sup>
				0.07–10 µg L <sup>-1</sup>	GC-ICP-MS/MS: foods <sup>60</sup>
Se <sup>+</sup> (77, 78, 80, 82)	Ar <sub>2</sub> <sup>+</sup> , Ar <sub>2</sub> H <sup>+</sup> , ArCa <sup>+</sup> , ArCl <sup>+</sup> , SO <sub>3</sub> <sup>+</sup>	H <sub>2</sub> (4)	Se <sup>+</sup>	11 nmol QDs L <sup>-1</sup> , 0.2 ng L <sup>-1</sup> (0.2 fmol))	FFF-ICP-MS/MS: quantum dots <sup>67,68,87</sup>
		O <sub>2</sub> (0.3–0.6)	SeO <sup>+</sup>	1 ng L <sup>-1</sup> ; 3 ng L <sup>-1</sup>	HNO <sub>3</sub> (1% v/v) <sup>26*</sup> ; silicon-containing minerals <sup>102</sup>
Se <sup>+</sup> (77, 78, 80, 82)	Ar <sub>2</sub> <sup>+</sup> , Ar <sub>2</sub> H <sup>+</sup> , ArCa <sup>+</sup> , ArCl <sup>+</sup> , SO <sub>3</sub> <sup>+</sup>	H <sub>2</sub> (4)	Se <sup>+</sup>	0.6–3 µg g <sup>-1</sup>	HPLC-ICP-MS/MS: cattle feed and beef, <sup>103</sup> dietary supplements <sup>104</sup>
		O <sub>2</sub> (0.3–0.6)	SeO <sup>+</sup>	0.004–1 ng g <sup>-1</sup> ; 2–100 ng L <sup>-1</sup> ; 9–34 nmol L <sup>-1</sup>	Tobacco <sup>78*</sup> ; crude oils <sup>79*</sup> ; food <sup>77*</sup> ; fed chickens <sup>97*</sup> ; food <sup>74*</sup> ; HgSe fluorescent nanoparticles, <sup>91</sup> biological samples (isotope dilution); <sup>50</sup> serum <sup>33</sup>
Se <sup>+</sup> (77, 78, 80, 82)	Ar <sub>2</sub> <sup>+</sup> , Ar <sub>2</sub> H <sup>+</sup> , ArCa <sup>+</sup> , ArCl <sup>+</sup> , SO <sub>3</sub> <sup>+</sup>	H <sub>2</sub> (4)	Se <sup>+</sup>	0.6 µg g <sup>-1</sup>	LA-ICP-MS/MS: prostate cancer biopsy sample <sup>71</sup>
		O <sub>2</sub> (0.3–0.6)	SeO <sup>+</sup>	1–3 µg kg <sup>-1</sup>	HPLC-ICP-MS/MS: selenoproteins in plasma (isotope dilution), <sup>66</sup> selenoproteins in rat serum <sup>105</sup>
Se <sup>+</sup> (77, 78, 80, 82)	Ar <sub>2</sub> <sup>+</sup> , Ar <sub>2</sub> H <sup>+</sup> , ArCa <sup>+</sup> , ArCl <sup>+</sup> , SO <sub>3</sub> <sup>+</sup>	H <sub>2</sub> (4)	Se <sup>+</sup>		FFF-ICP-MS/MS: quantum dots <sup>67,68,87</sup>
		O <sub>2</sub> (0.3–0.6)	SeO <sup>+</sup>		

Table 2 (Contd.)

Analyte ion (nuclide mass)	Potential interfering ion(s) <sup>a</sup>	Reaction gas (mL min <sup>-1</sup> )	Measured ion	LoDs <sup>b</sup>	Additional information
Si <sup>+</sup> (28, 29, 30)	CO <sup>+</sup> , N <sub>2</sub> <sup>+</sup> , N <sub>2</sub> H <sup>+</sup> , NO <sup>+</sup>	CH <sub>3</sub> F (1.0) H <sub>2</sub> (10) O <sub>2</sub> (0.5) O <sub>2</sub> (0.2–1)	SeCH <sub>2</sub> <sup>+</sup> Si <sup>+</sup> Si <sup>+</sup> SiO <sup>+</sup>	11 nmol QDs L <sup>-1</sup> , 0.2 ng L <sup>-1</sup> (0.2 fmol) 4–10 ng L <sup>-1</sup> 0.1–69 µg L <sup>-1</sup> 0.2 ng L <sup>-1</sup> 0.5–1 µg L <sup>-1</sup>	Environmental samples <sup>41</sup> FFF-ICP-MS/MS: silica nanoparticles <sup>69</sup> HNO <sub>3</sub> (1% v/v) <sup>26*</sup> (Bio)diesel and oil <sup>93*</sup> , nuclear waste glasses <sup>106</sup> FFF-ICP-MS/MS: silica nanoparticles <sup>69</sup> Sediments, fertilizer and sludge <sup>45*</sup> HNO <sub>3</sub> (1% v/v) <sup>26*</sup> LA-ICP-MS/MS: magmatic rocks (isotopic analysis) <sup>107</sup> Whole blood <sup>48*</sup> , geological material (isotopic analysis) <sup>59</sup> LA-ICP-MS/MS: glass type geological material (isotopic analysis) <sup>72</sup> Minerals (isotopic analysis) <sup>86</sup> HNO <sub>3</sub> (1% v/v) <sup>26*</sup> ; crude oils <sup>79*</sup> ; carbonates <sup>43*</sup> Blood serum, <sup>36</sup> TiO <sub>2</sub> nanoparticles <sup>70</sup> LA-ICP-MS/MS: high pressure rutile-quartz veins <sup>108</sup> Biofluids <sup>47*,48*</sup> Environmental samples <sup>109,110</sup> HNO <sub>3</sub> (1% v/v) <sup>26*</sup> , drinking water <sup>42*</sup> ; crude oils <sup>79*</sup> Biofluids <sup>47*,48*</sup> HNO <sub>3</sub> (1% v/v) <sup>26*</sup>
Sn <sup>+</sup> (120)	PdO <sup>+</sup> , RuO <sup>+</sup> , Te <sup>+</sup>	O <sub>2</sub> (0.3)	Sn <sup>+</sup>	0.1–0.6 µg L <sup>-1</sup>	
Sr <sup>+</sup> (86, 87, 88)	ArCa <sup>+</sup> , ArCr <sup>+</sup> , ArTi <sup>+</sup> , GeO <sup>+</sup> , Hf <sup>+</sup> , Yb <sup>++</sup>	O <sub>2</sub> (0.5) O <sub>2</sub> (0.25)	Sr <sup>+</sup> SrO <sup>+</sup>	9 ng g <sup>-1</sup> 6 ng L <sup>-1</sup> N.A.	
		CH <sub>3</sub> F (0.9)	SrF <sup>+</sup>	0.5–1 ng L <sup>-1</sup>	
Ti <sup>+</sup> (46, 47, 48, 49, 50)	ArC <sup>+</sup> , ArCH <sup>+</sup> , ArN <sup>+</sup> , C <sub>4</sub> <sup>+</sup> , CCl <sup>+</sup> , ClN <sup>+</sup> , ClNH <sup>+</sup> , N <sub>2</sub> O <sup>+</sup> , NO <sub>2</sub> <sup>+</sup> , NO <sub>2</sub> H <sup>+</sup> , PO <sup>+</sup> , POH <sup>+</sup> , SiOH <sup>+</sup> , SN <sup>+</sup> , SNH <sup>+</sup> , SO <sup>+</sup> , SOH <sup>+</sup>	SF <sub>6</sub> /H <sub>2</sub> (0.03/5) O <sub>2</sub> (0.1–0.3)	SrF <sup>+</sup> TiO <sup>+</sup>	N.A. 4 ng L <sup>-1</sup> ; 7 pg g <sup>-1</sup> ; N.A.	
		NH <sub>3</sub> (2) NH <sub>3</sub> (N.A.)	Ti(NH <sub>3</sub> ) <sub>6</sub> <sup>+</sup> TiNH(NH <sub>3</sub> ) <sub>4</sub> <sup>+</sup>	3–10 ng L <sup>-1</sup> 0.01–0.5 µg g <sup>-1</sup>	
U <sup>+</sup> (236, 238)	UH <sup>+</sup>	CH <sub>3</sub> F (0.9–1) O <sub>2</sub> (0.1)	TiF <sub>2</sub> (CH <sub>3</sub> F) <sub>3</sub> <sup>+</sup> UO <sup>+</sup>	1–3 ng L <sup>-1</sup> N.A.	
V <sup>+</sup> (51)	ArC <sup>+</sup> , ArN <sup>+</sup> , ArNH <sup>+</sup> , ClN <sup>+</sup> , ClO <sup>+</sup> , SN <sup>+</sup> , SO <sup>+</sup> , SOH <sup>+</sup>	O <sub>2</sub> (0.1–0.3)	VO <sup>+</sup>	2 ng L <sup>-1</sup> ; 0.3 pg g <sup>-1</sup>	
Y <sup>+</sup> (89)	ArTi <sup>+</sup> , ArCr <sup>+</sup> , ArV <sup>+</sup> , GaO <sup>+</sup> , GeO <sup>+</sup> , Hf <sup>++</sup>	CH <sub>3</sub> F (0.8–1) O <sub>2</sub> (0.1)	VF <sub>2</sub> (CH <sub>3</sub> F) <sub>3</sub> <sup>+</sup> YO <sup>+</sup>	0.1 ng L <sup>-1</sup> 0.4 ng L <sup>-1</sup>	
Zn <sup>+</sup> (66)	S <sub>2</sub> <sup>+</sup> , SO <sub>2</sub> <sup>+</sup> , SO <sub>2</sub> H <sup>+</sup> , TiO <sup>+</sup>	O <sub>2</sub> (0.3–0.6)	Zn <sup>+</sup>	2.5 µg g <sup>-1</sup>	LA-ICP-MS/MS: prostate cancer biopsy sample <sup>71</sup>
		NH <sub>3</sub> (3)	Zn(NH <sub>3</sub> ) <sub>2</sub> <sup>+</sup>	11 nmol QDs L <sup>-1</sup> , 0.2 ng L <sup>-1</sup> (0.2 fmol)	FFF-ICP-MS/MS: quantum dots <sup>67,68,87</sup>
Zr <sup>+</sup> (90, 91)	ArCr <sup>+</sup> , ArTi <sup>+</sup> , ArV <sup>+</sup> , AsO <sup>+</sup> , GeO <sup>+</sup> , Hf <sup>++</sup> , W <sup>++</sup>	CH <sub>3</sub> F (1)	ZrF <sup>+</sup>	150 pg g <sup>-1</sup> 6–10 ng L <sup>-1</sup>	Crude oils <sup>79*</sup> Whole blood <sup>48*</sup>

<sup>a</sup> Potentially interfering ions (non-restrictive list). <sup>b</sup> Instrumental or methodological limits of detection (see the corresponding reference for further information). \*Multi-element method. N.A. = not available.

approach). Böting *et al.*<sup>35</sup> have evaluated the performance of this reaction for the indirect measurement of several target analytes (As, Au, B, Be, Br, Cl, I, P and Se) at  $m/z = 32$ . These authors demonstrated using isotopically enriched O<sub>2</sub> that asymmetric charge transfer also occurs for elements with lower ionization energy (*i.e.*, when the reaction is not likely to occur), and they have tentatively explained that the reaction proceeds through metastable ionic states. Further investigation is, however, required to fully explain the processes observed.

Although O<sub>2</sub> has been widely used, both in ICP-QMS and in ICP-MS/MS, two important drawbacks of this reaction gas need to be pointed out. On one hand, the O-atom transfer may impose difficulties to resolve isobaric overlap for those elements (analyte and interfering elements) with a similar affinity towards O<sub>2</sub>. Those elements typically react in the same way and thus, the reaction product ions of the analyte and the interfering ions have the same  $m/z$ . Also for analyte signals that

show spectral overlap with that of an O-based polyatomic interference *i.e.*,  $m/z A^+ = m/z IO^+$ , the addition of O<sub>2</sub> in the cell might lead to the formation of the reaction product ions AO<sup>+</sup> and IO<sub>2</sub><sup>+</sup>, the signals of which will overlap at the new  $m/z$ .

The use of highly reactive gases, as for instance NH<sub>3</sub>, can be seen as an elegant alternative to solve this kind of interferences. An example of this approach was shown by Balcaen *et al.*<sup>36</sup> This work aimed at the determination of ultra-trace levels of titanium (Ti) in blood serum in order to evaluate the condition of Ti-based implants in the human body. The capabilities of O<sub>2</sub> and NH<sub>3</sub> to resolve the spectral overlap for different Ti isotopes (caused by the occurrence of *e.g.*, Ca<sup>+</sup>, PO<sup>+</sup> and SO<sup>+</sup>) were evaluated. The best suited reaction product ions were identified *via* product ion scanning (see Fig. 8). The product ion scans for <sup>48</sup>Ti<sup>+</sup> in the presence of <sup>48</sup>Ca<sup>+</sup> using O<sub>2</sub> (Fig. 8A) and NH<sub>3</sub> (Fig. 8B) show the different behavior of those gases. TiO<sup>+</sup>, and to a much lesser extent TiO<sub>2</sub><sup>+</sup>, were formed by reaction with O<sub>2</sub>,

**Table 3** S-Isotopes with their natural isotopic abundance and the most important potentially interfering ions hampering accurate S determination

Analyte	Abundance (%)	Ions causing spectral interference
$^{32}\text{S}^+$	95.04	$^{16}\text{O}^{16}\text{O}^+$ , $^{14}\text{N}^{18}\text{O}^+$ , $^{15}\text{N}^{16}\text{O}^1\text{H}^+$
$^{33}\text{S}^+$	0.75	$^{32}\text{S}^1\text{H}^+$ , $^{16}\text{O}^{16}\text{O}^1\text{H}^+$ , $^{16}\text{O}^{17}\text{O}^+$ , $^{15}\text{N}^{18}\text{O}^+$ , $^{14}\text{N}^{18}\text{O}^1\text{H}^+$
$^{34}\text{S}^+$	4.20	$^{33}\text{S}^1\text{H}^+$ , $^{16}\text{O}^{18}\text{O}^+$
$^{32}\text{S}^{16}\text{O}^+$	95.04	$^{48}\text{Ti}^+$ , $^{48}\text{Ca}^+$ , $^{36}\text{Ar}^{12}\text{C}^+$
$^{33}\text{S}^{16}\text{O}^+$	0.75	$^{49}\text{Ti}^+$ , $^{32}\text{S}^{17}\text{O}^+$
$^{34}\text{S}^{16}\text{O}^+$	4.20	$^{50}\text{Ti}^+$ , $^{50}\text{Cr}^+$ , $^{50}\text{V}^+$ , $^{38}\text{Ar}^{12}\text{C}^+$ , $^{36}\text{Ar}^{14}\text{N}^+$ , $^{32}\text{S}^{18}\text{O}^+$ , $^{33}\text{S}^{17}\text{O}^+$

whereas for  $\text{NH}_3$ , higher order reaction product ions were also observed. The isobaric interference of  $^{48}\text{Ca}^+$  and  $^{48}\text{Ti}^+$  cannot be overcome by means of  $\text{O}_2$ , despite the reaction between Ca and  $\text{O}_2$  being an endothermic process that should theoretically not proceed in the cell. In practice however, this reaction proceeds to some extent as a result of the large excess of Ca in biological fluids. However, owing to the difference in reactivity between Ti and Ca towards  $\text{NH}_3$ , the isobaric overlap can be overcome. For Ti, a higher order reaction product ion ( $\text{Ti}(\text{NH}_3)_6^+$ ) is formed, the signal of which is free from Ca-based spectral overlap. In addition, when using  $\text{O}_2$ , it was also demonstrated that the presence of high amounts of S and P in biofluids may give rise to spectral interferences for some Ti isotopes, due to the formation of  $\text{SO}^+$  and  $\text{PO}^+$  in the plasma source that are able to reach the cell and pass Q2 as  $\text{SO}_2^+$  and  $\text{PO}_2^+$ , overlapping with the signals of  $^{47}\text{TiO}^+$  and  $^{49}\text{TiO}^+$ , respectively. A problem which can also be avoided by using  $\text{NH}_3$ . Thus, the mass-shift approach using  $\text{NH}_3$  gas was considered more suitable for the determination of ultra-traces of Ti in biological samples, and instrumental LODs in the order of  $10\text{ ng L}^{-1}$  were realized.

In addition to the gases most commonly used in ICP-MS/MS, *i.e.*,  $\text{H}_2$ , He,  $\text{NH}_3$  and  $\text{O}_2$ , also methyl fluoride ( $\text{CH}_3\text{F}$ ) has been evaluated for its capabilities as a reaction gas to avoid spectral

overlap. This highly reactive gas has only been used scarcely in ICP-MS before,<sup>37,38</sup> but with the introduction of ICP-MS/MS, its application range has been systematically extended. Like for  $\text{NH}_3$ ,  $\text{CH}_3\text{F}$  reacts with the analyte ion (mass-shift approaches) in many different ways, to produce both simple and higher order reaction product ions. According to literature,<sup>39,40</sup> F-atom transfer ( $\text{AF}^+$ ),  $\text{CH}_3\text{F}$  addition ( $\text{ACH}_3\text{F}^+$ ) and  $\text{CH}_3\text{F}$  addition followed by  $\text{HF}$  ( $\text{ACH}_2^+$ ) or  $\text{H}_2$  ( $\text{ACHF}^+$ ) elimination, are the most prevalent reaction pathways, but also the combination of those reactions to produce higher order reaction product ions has been reported on ( $\text{AF}_a(\text{CH}_b\text{F}_c)_d^+$ ). Bolea-Fernandez *et al.*<sup>41</sup> describe the use of  $\text{CH}_3\text{F}$  (more accurately a mixture of 10%  $\text{CH}_3\text{F}$  and 90% He) for the mono-element determination of ultra-trace concentrations of As and Se. It was observed that, a selective reaction between the target nuclides  $^{75}\text{As}$  and  $^{77,78,80}\text{Se}$  takes place in the CRC to produce  $^{75}\text{AsCH}_2^+$  ( $m/z = 89$ ) and  $^{77,78,80}\text{SeCH}_2^+$  ( $m/z = 91, 92$  and  $94$ , respectively). These methods with different reaction gas flow rates for As and Se were successfully applied for the interference-free determination of As and Se in reference materials of plant, animal and environmental origin. Instrumental LODs of  $0.2\text{ ng L}^{-1}$  for  $^{75}\text{As}$  and  $\leq 10\text{ ng L}^{-1}$  for  $^{77,78,80}\text{Se}$  were obtained, which are according to the best of the authors' knowledge, the lowest LODs reported on in the literature for these elements by means of ICP-MS so far. However, despite of the benefits of  $\text{CH}_3\text{F}$  (*e.g.*, highly reactive, but non-corrosive gas) as a reaction gas for ICP-MS/MS, also some disadvantages have to be noted, such as the requirement for additional safety measures and the fact that – until the introduction of the second generation of ICP-MS/MS in 2016 – this gas was not part of the standard set of gases recommended for such a type of instrumentation.

**3.1.2. Multi-elemental analysis.** While the specificity of some of the reactions taking place in the reaction cell may often be seen as positive, it may also be considered as a limitation for multi-element approaches. Generally seen, multi-element determination is an important advantage of ICP-MS over other analytical techniques. Simultaneous (as in 'during the same measurement')

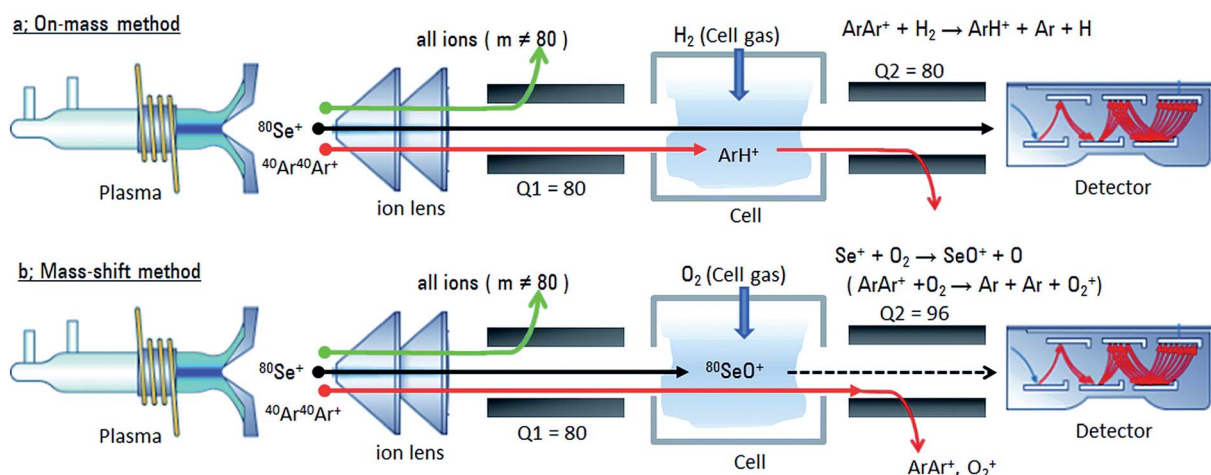


**Fig. 7** Example of on-mass (a) and mass-shift (b) approaches for the interference-free determination of  $^{80}\text{Se}$  using ICP-MS/MS operated in MS/MS mode. From Sugiyama *et al.*<sup>34</sup>

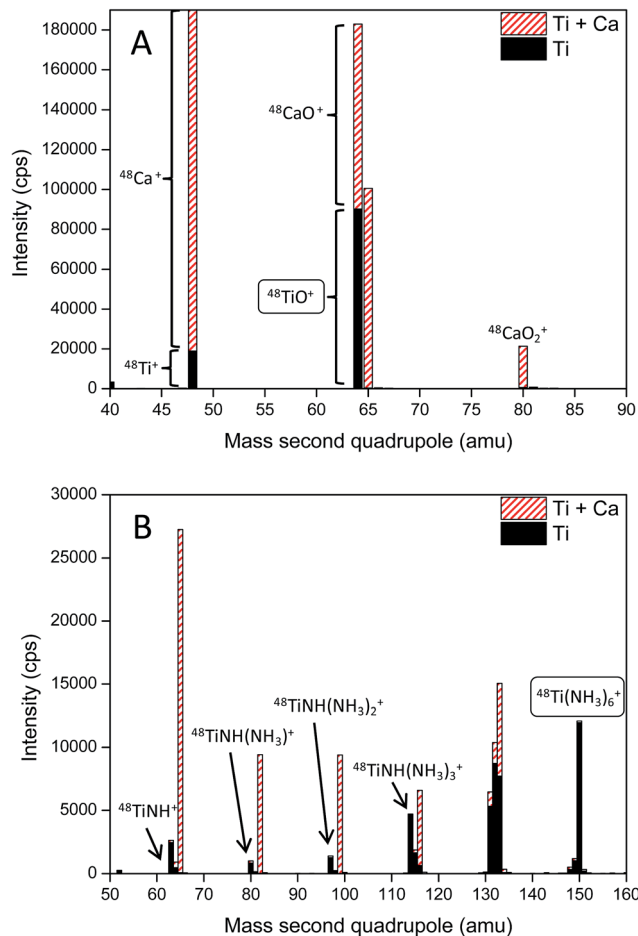


Fig. 8 Product ion scans with Q1 fixed at  $m/z = 48$  for a solution containing  $1 \mu\text{g L}^{-1}$  Ti and a solution containing  $1 \mu\text{g L}^{-1}$  Ti +  $10 \text{ mg L}^{-1}$  Ca. The reaction gas selected was  $\text{O}_2$  ( $0.2 \text{ mL min}^{-1}$  – A) and  $\text{NH}_3$  ( $2 \text{ mL min}^{-1}$   $\text{NH}_3/\text{He}$  – B). Adapted from Balcaen *et al.*<sup>36</sup>

determination is especially relevant when aiming at high sample throughput, when the amount of sample is limited or when monitoring short transient signals. Below, specific applications aiming at ICP-MS/MS multi-element analysis are described.

$\text{O}_2$  has been widely used for the simultaneous determination of several analyte elements by means of ICP-MS/MS, usually making use of the combination of on-mass and mass-shift approaches within the same method. In this way, the determination of As, Cr, Hg and V in drinking water was accomplished by Amaral *et al.*<sup>42</sup> O-atom transfer in a mass-shift approach was relied on to avoid the spectral overlap (e.g.  $^{40}\text{Ar}^{35}\text{Cl}^+$ ,  $^{35}\text{Cl}^{17}\text{O}^+$  and  $^{35}\text{Cl}^{16}\text{O}^+$ ) affecting As, Cr and V *via* monitoring of the reaction product ions  $\text{AsO}^+$ ,  $\text{CrO}^+$  and  $\text{VO}^+$ , while Hg was determined on-mass under the same analytical conditions (owing to the absence of strong spectral interferences and to the low reactivity towards  $\text{O}_2$ ). For this application,  $0.3 \text{ mL min}^{-1}$  of  $\text{O}_2$  sufficed to avoid spectral overlap and LODs of 2, 3, 2 and  $40 \text{ ng L}^{-1}$  could be obtained for V (as  $^{51}\text{V}^{16}\text{O}^+$ ), Cr (as  $^{52}\text{Cr}^{16}\text{O}^+$ ), As (as  $^{75}\text{As}^{16}\text{O}^+$ ) and Hg (as  $^{202}\text{Hg}^+$ ), respectively.

The combination of on-mass and mass-shift approaches was also used by Diez Fernández *et al.*<sup>43</sup> for the determination of

P/Ca, S/Ca and low B/Ca ratios in carbonates. O-atom transfer was used for the determination of P and S as the corresponding  $\text{PO}^+$  and  $\text{SO}^+$  reaction product ions. However, special attention was also paid to the interferences affecting B and Ca, and to the way to resolve them. Firstly, because of the high concentration of Ca in comparison to B, the least abundant Ca isotope, *i.e.*  $^{46}\text{Ca}$ , was selected in order to be able to detect both elements in pulse counting mode. The overlap of  $^{46}\text{Ti}^+$  and  $^{46}\text{Ca}^+$  was taken care of by converting  $^{46}\text{Ti}$  ions into the corresponding  $^{46}\text{TiO}^+$  ions, while  $^{46}\text{Ca}^+$  can be measured on-mass due to the low reactivity of Ca towards  $\text{O}_2$ . For B, the situation is rather different, as the determination of  $^{11}\text{B}$  is affected by the strong signal of the ubiquitous  $^{12}\text{C}$ , potentially leading to inaccurate (biased high) results due to the overlap of the  $^{12}\text{C}^+$  signal tail with the signal of  $^{11}\text{B}^+$ . The improvement in abundance sensitivity realized by operating the ICP-tandem mass spectrometer in MS/MS mode allowed for a full separation of the signals of  $^{11}\text{B}$  and  $^{12}\text{C}$  (see Fig. 9), in contrast to conventional ICP-QMS or ICP-MS/MS operating in SQ mode. The method developed was successfully applied to the measurement of low B/Ca ratios in

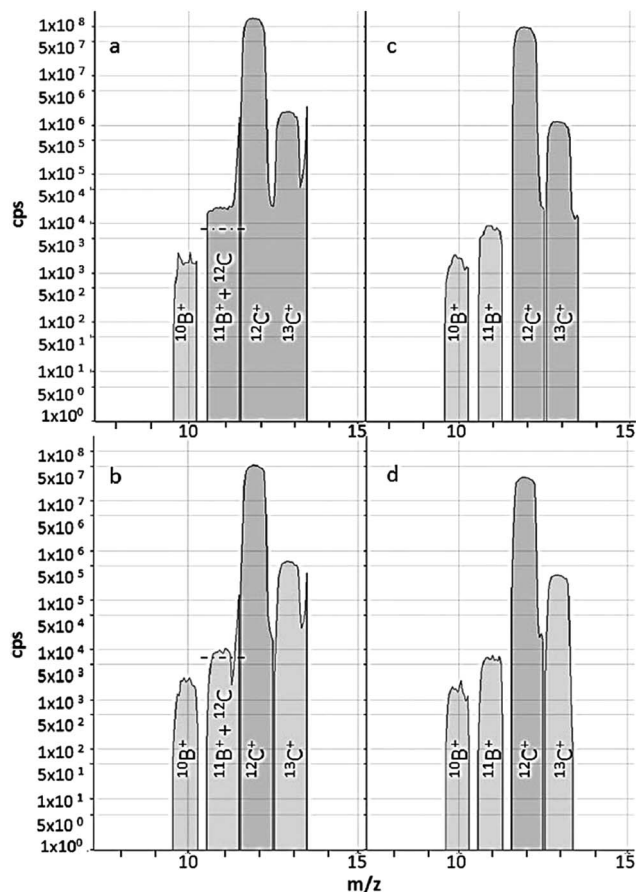


Fig. 9 Example of the enhanced abundance sensitivity for ICP-MS/MS operated in MS/MS mode over SQ mode. The figure shows the mass spectra obtained for  $0.5 \text{ ppb B}$  using: SQ mode in (a)  $1.3$  and (b)  $0.1 \text{ mg carbonate mL}^{-1}$  solution and MS/MS mode in (c)  $1.3$  and (d)  $0.1 \text{ mg carbonate mL}^{-1}$  solution. (a and b) show the influence of the  $^{12}\text{C}^+$  signal tail on the signal of  $^{11}\text{B}^+$ . From Diaz Fernández *et al.*<sup>43</sup>

samples with high C content, such as carbonates, which can be used to study ocean acidification.

Amatis *et al.*<sup>44</sup> have made use of O<sub>2</sub> to avoid MoO<sup>+</sup> interferences in the determination of Cd in milk. As MoO<sup>+</sup> ions formed in the plasma source exhibit the same *m/z* as Cd ions, they enter the cell together. However, the introduction of 0.5 mL min<sup>-1</sup> of O<sub>2</sub> enables to convert the MoO<sup>+</sup> ions into the corresponding MoO<sub>2</sub><sup>+</sup> ions, while Cd shows no reactivity towards O<sub>2</sub>, thus allowing interference-free determination of Cd (on-mass approach) and of Mo (as MoO<sub>2</sub><sup>+</sup> – mass-shift approach).

Such a combination of on-mass and mass-shift approaches was also used by Machado *et al.*<sup>45</sup> aiming at obtaining interference-free conditions enabling for the simultaneous determination of Cd, Pd, Pt, Rh and Sn in complex matrices *i.e.* sediments, fertilizer and sludge samples. By means of the use of O<sub>2</sub> (0.3 mL min<sup>-1</sup>) in MS/MS mode, <sup>106</sup>Pd<sup>+</sup>, <sup>112</sup>Cd<sup>+</sup> and <sup>120</sup>Sn<sup>+</sup> ions were measured on-mass, while <sup>103</sup>Rh<sup>+</sup> and <sup>195</sup>Pt<sup>+</sup> ions were converted into <sup>103</sup>Rh<sup>16</sup>O<sup>+</sup> and <sup>195</sup>Pt<sup>16</sup>O<sup>+</sup> reaction product ions and were measured after mass-shift. LODs of 2, 10, 15, 2.5 and 9 µg kg<sup>-1</sup> were reported for Cd, Pd, Pt, Rh and Sn, respectively. Quantitative recoveries (80–117%) after addition of 0.5, 1.0 and 5.0 µg L<sup>-1</sup> of the target analytes were obtained using the corresponding on-mass and mass-shift O<sub>2</sub>-MS/MS approaches.

In contrast to O<sub>2</sub>, the high reactivity of NH<sub>3</sub> leads to many simple and higher order reaction product ions, which renders it into a potentially powerful tool for multi-element method development. An example demonstrating the capabilities of NH<sub>3</sub> for multi-elemental analysis was provided by Sugiyama *et al.*<sup>34</sup> in the context of the interference-free determination of noble metal elements – Ag, Au, Ir, Pd, Pt, Os, Rh and Ru. Noble metals comprise the platinum group metals (PGMs), Au and Ag, and are highly affected by several types of interferences. The high reactivity of NH<sub>3</sub> towards many of these interferences was used for avoiding spectral overlap. Ag, Pd, Rh and Ru show low reactivity with NH<sub>3</sub>, so upon removing the interfering ions by reaction with NH<sub>3</sub>, these analyte elements could be accurately measured at their original *m/z* (on-mass approach). In the case of Au, Ir, Os and Pt, high reactivity was shown for both analyte and interfering ions. Thus, the best suited reaction product ions were identified *via* product ion scanning. By means of the comparison of the corresponding product ion spectra for analyte and interfering ions, Au(NH<sub>3</sub>)<sub>2</sub><sup>+</sup>, IrNH<sup>+</sup>, OsNH<sup>+</sup> and Pt(NH<sub>3</sub>)<sub>2</sub><sup>+</sup> were selected for quantification purposes (mass-shift approach).

A further evaluation of the reactivity of Pd, Pt and Rh with NH<sub>3</sub> gas (3 mL min<sup>-1</sup>) was performed by Suoranta *et al.*<sup>46</sup> for the analysis of moss samples. It was demonstrated that, in the presence of higher concentrations of possible interfering elements, the best approach (on-mass and/or mass-shift) and the more suited reaction product ions need to be carefully selected, taking into account the interferences affecting every isotope or reaction product ion thereof. In this specific case of study, Rh was determined either using an on-mass (<sup>103</sup>Rh<sup>+</sup>) or mass-shift (<sup>103</sup>Rh(NH<sub>3</sub>)<sub>4</sub><sup>+</sup>) approach. However, interference-free conditions for the determination of Pd were reached using the reaction product ion <sup>108</sup>Pd(NH<sub>3</sub>)<sub>3</sub><sup>+</sup> only, while the results obtained using the other Pd isotopes were clearly biased high. Pt was determined using the reaction product ion Pt(NH<sub>3</sub>)<sub>2</sub><sup>+</sup>. This

example gives an idea about the potential of ICP-MS/MS in combination with highly reactive gases to avoid spectral overlap in the most demanding applications *i.e.* very high concentrations of interfering elements and ultra-trace levels of the target nuclides.

Next to NH<sub>3</sub>, also CH<sub>3</sub>F (a mixture of 10% CH<sub>3</sub>F and 90% He) has been evaluated for its capabilities for multi-elemental analysis. The potential of CH<sub>3</sub>F in ICP-MS/MS was assessed by Bolea-Fernandez *et al.*<sup>47</sup> in the context of the determination of ultra-trace concentrations of light metals (*m/z* ≤ 60) in bio-fluids. Al, Co, Cr, Mn, Ni, Ti and V were selected as the target elements due to their relevance in biomedical applications. It was observed that low CH<sub>3</sub>F/He gas flow rates preferentially lead to F-atom transfer (AF<sup>+</sup>), while higher gas flow rates rather lead to CH<sub>3</sub>F addition (A(CH<sub>3</sub>F)<sub>x</sub><sup>+</sup>) and/or higher order reaction product ions (AF<sub>a</sub>(CH<sub>3</sub>F)<sub>b</sub><sup>+</sup>). *Via* product ion scanning, the best reaction product ions were identified. Under compromise conditions (*i.e.* maximum CH<sub>3</sub>F/He gas flow rate – 1 mL min<sup>-1</sup> with the mass flow controller calibrated for O<sub>2</sub>), a multi-element method was developed for the simultaneous determination of all target elements. Accurate results were obtained, with LODs below 10 ng L<sup>-1</sup>.

The multi-element capabilities shown by CH<sub>3</sub>F gas were further exploited for the determination of ultra-trace concentrations of prosthesis-related metals (Al, Ti, V, Co, Cr, Ni, Sr and Zr) in whole blood.<sup>48</sup> The accuracy of the ICP-MS/MS method developed was demonstrated *via* successful analysis of whole blood reference materials, and of real venous blood samples spiked with the target elements at different concentration levels (5 to 50 µg L<sup>-1</sup>). In combination with volumetric absorptive micro-sampling (VAMS), sample volumes as low as 10 µL could be subjected to multi-elemental assay.

### 3.2. Isotopic analysis

As is widely known, ICP-MS is not only able to provide elemental, but also isotopic information. These isotope ratio measurements can even be affected by spectral interference to a larger extent, as for this type of analysis at least two isotopes of the same element need to be measured interference-free. In addition, while a bias of 1% might be negligible in elemental assay, it biases isotope ratio data far beyond acceptable limits. The use of ICP-MS/MS for both the determination of natural variations in isotopic composition and for isotope dilution mass spectrometry (IDMS) have been reported on in literature.

**3.2.1. Isotope dilution mass spectrometry.** IDMS is considered as one of the most powerful methods for elemental assay with high accuracy.<sup>49</sup> The capabilities of ICP-MS/MS for IDMS determination of S (*via* monitoring of the SO<sup>+</sup> reaction product ions) in organic matrices were evaluated by Balcaen *et al.*<sup>31</sup> However, the presence of interfering ions at the *m/z* of the reaction product ions selected (Ca<sup>+</sup>, Cr<sup>+</sup>, Ti<sup>+</sup> and – in organic matrix – also ArC<sup>+</sup>) traditionally jeopardizes accurate determination. For evaluating the potential of ICP-MS/MS, 3 different modes were used: standard mode (no gas), bandpass mode (simulating ICP-DRC-QMS conditions) and MS/MS mode (see Fig. 10). It was clear that only when using the MS/MS mode, accurate results can

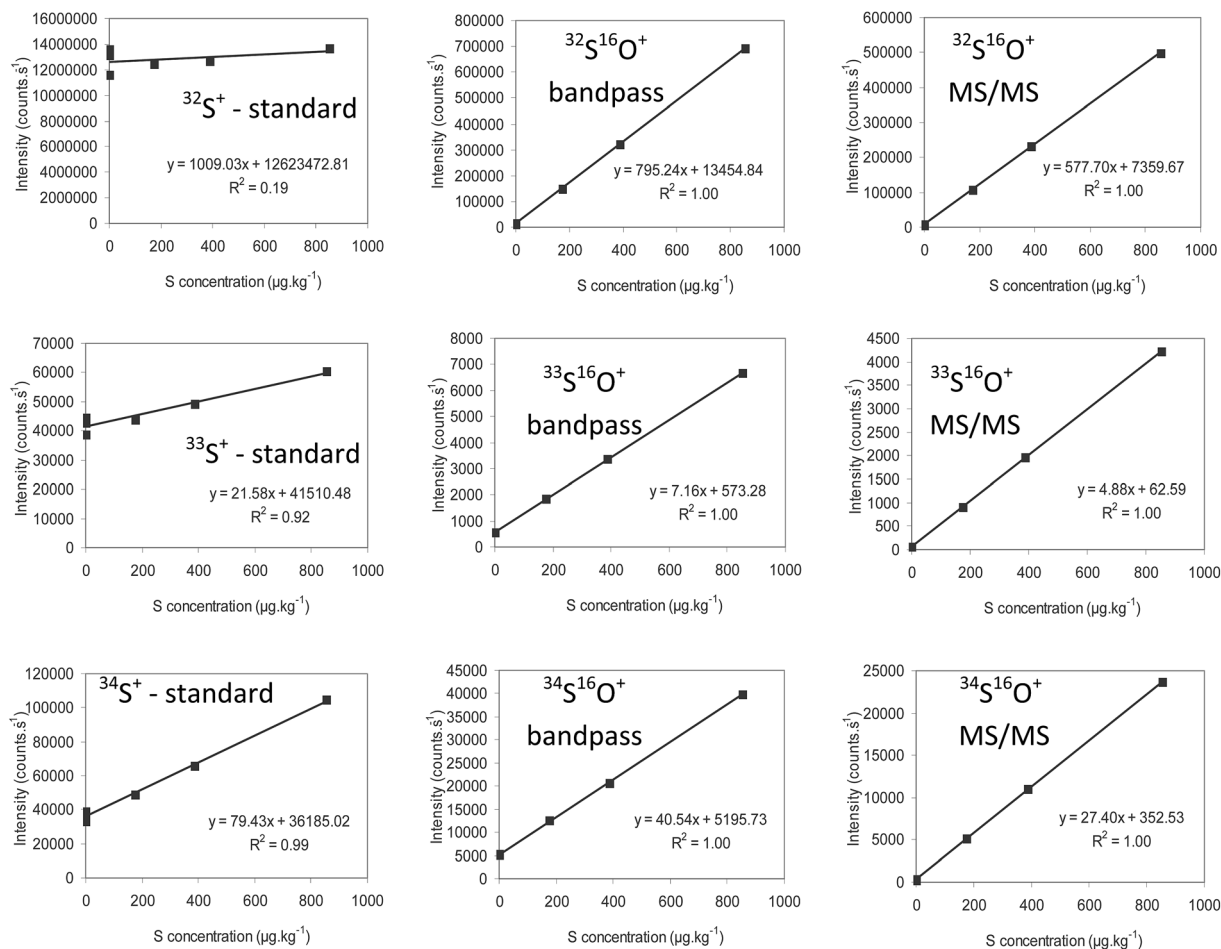


Fig. 10 Calibration curves obtained for  $^{32}\text{S}^+$ ,  $^{33}\text{S}^+$  and  $^{34}\text{S}^+$  (standard mode) and  $^{32}\text{S}^{16}\text{O}^+$ ,  $^{33}\text{S}^{16}\text{O}^+$  and  $^{34}\text{S}^{16}\text{O}^+$  (bandpass mode and MS/MS mode) for a series of standards with concentrations ranging between 0 and 850  $\mu\text{g kg}^{-1}$ . From Balcaen *et al.*<sup>31</sup>

be obtained by means of IDMS. As a proof-of-concept, S was successfully determined in the NIST SRM 2773 (biodiesel) reference material. A general method for the accurate quantification of S in organic matrices was provided, which is also applicable to S-speciation *via* reverse phase HPLC-ICP-MS/MS.

Another example of ID-ICP-MS/MS was described by Bamonti *et al.*<sup>50</sup> In this work, accurate high-throughput quantification of Se in biological samples was aimed at. The approach developed was based on the combination of on-line isotope dilution by means of flow injection and the use of H<sub>2</sub> (on-mass) or O<sub>2</sub> (mass-shift) to avoid spectral overlap *via* ICP-MS/MS operated in MS/MS mode. The on-line approach was compared with direct infusion followed by IDMS. Interference-free conditions were reached for the measurement of <sup>77,78,80,82</sup>Se isotopes as <sup>77,78,80,82</sup>SeO<sup>+</sup> reaction product ions, while the use of H<sub>2</sub> (combined with kinetic energy discrimination - KED) resulted in an increased background for <sup>82</sup>Se, thus preventing the use of this nuclide when the instrument is operated in H<sub>2</sub>-KED mode. The approaches developed were evaluated *via* the measurement of a certified reference material and 10 real serum samples. The results showed the potential of ID-ICP-MS/MS for the determination of Se concentrations with

high throughput, allowing the measurement of serum in  $\mu\text{L}$ -sample volumes.

**3.2.2. Natural variations in isotopic composition.** In isotopic analysis, high precision is required to reveal the often small natural variations in isotopic compositions. For this reason, the use of ICP-QMS has often been restricted to the study of induced changes in the isotopic composition of target elements in the context of tracer experiments with enriched stable isotopes or of IDMS. However, although limited to values of  $\sim 0.1\%$  RSD, the precision attainable by means of quadrupole-based ICP-MS instrumentation is fit-for-purpose for the study of natural variations in some specific applications, especially those dealing with elements with (a) radiogenic nuclide(s).

An ICP-MS/MS method for the accurate determination of <sup>129</sup>I/<sup>127</sup>I isotope ratios was developed by Ohno *et al.*<sup>51</sup> with the objective of investigating radioiodine released by the Fukushima Daiichi Nuclear Power Plant (FDNPP) accident. However, the ultra-trace concentrations of <sup>129</sup>I<sup>+</sup> and the overlap of this signal with that of the isobaric <sup>129</sup>Xe<sup>+</sup> and with the polyatomic ions <sup>127</sup>IH<sub>2</sub><sup>+</sup> and <sup>127</sup>ID<sup>+</sup> might hinder this determination. The use of 0.9 mL min<sup>-1</sup> of O<sub>2</sub> in the reaction cell was sufficient to

obtain a 1000-fold improvement in the background equivalent concentration (BEC) by means of the reduction of the isobaric overlap by  $^{129}\text{Xe}^+$  (charge transfer). The low level of  $^{127}\text{IH}_2^+$  and  $^{127}\text{ID}^+$  formed in the plasma can be corrected for by mathematical correction.

In the aftermath of the Fukushima accident, some works have focused on the determination of cesium (Cs) isotope ratios.<sup>52–58</sup> The accurate determination of  $^{134}\text{Cs}/^{137}\text{Cs}$  and  $^{135}\text{Cs}/^{137}\text{Cs}$  ratios is hampered by the overlap of the signals of  $\text{Cs}^+$  with those of  $\text{Ba}^+$  and of the oxides of  $\text{Sb}^+$  and  $\text{Sn}^+$ . By means of ICP-MS/MS using nitrous oxide ( $\text{N}_2\text{O}$ ) as a reaction gas, accurate isotope ratio results were obtained for different environmental samples.  $\text{N}_2\text{O}$  is a non-common reactive gas for ICP-MS/MS, for which O-atom transfer is the main reaction. In these works, isobaric interferences from  $^{134,134,137}\text{Ba}$  were removed by means of reaction with  $\text{N}_2\text{O}$  ( $\text{Ba}^+ + \text{N}_2\text{O} \rightarrow \text{BaO}^+ + \text{N}_2$ ), while Cs isotopes can be measured free from spectral overlap at the original  $m/z$  (on-mass approach). In addition, the ICP-tandem mass spectrometer operating in the MS/MS mode is able to reject  $\text{Sb}^+$  and  $\text{Sn}^+$  ions by means of Q1, thus avoiding the formation of the interfering ions  $\text{SbO}^+$  and  $\text{SnO}^+$  by reaction with  $\text{N}_2\text{O}$  in the CRC. Thus, accurate isotopic analysis of Cs became feasible in spite of the different spectral interferences originally hindering this determination.

Another example of the use of ICP-tandem mass spectrometry for isotopic analysis is the measurement of strontium (Sr) isotope ratios. Sr shows relatively large natural variation in its isotopic composition as a result of the radiogenic character of  $^{87}\text{Sr}$ , *i.e.*  $\beta^-$  decay of  $^{87}\text{Rb}$  results in the formation of  $^{87}\text{Sr}$ . However,  $^{87}\text{Rb}$  shows isobaric overlap with  $^{87}\text{Sr}$ , such that accurate isotope ratio results cannot be obtained except if Sr is chemically separated from Rb prior to the analysis. Bolea-Fernandez *et al.*<sup>59</sup> used ICP-MS/MS and  $\text{CH}_3\text{F}/\text{He}$  as a reaction gas to avoid the spectral overlap in the isotopic analysis of Sr, by means of the reaction between  $\text{Sr}^+$  and  $\text{CH}_3\text{F}$ , leading to  $\text{SrF}^+$ , and the absence of reactivity in the case of Rb. Accurate  $^{87}\text{Sr}/^{86}\text{Sr}$  isotope ratio results (measured as  $^{87}\text{SrF}^+/^{86}\text{SrF}^+$ ) were obtained without matrix-matching of the external standard, and in the presence of interfering ions at the  $m/z$  of the reaction product ions selected, (owing to the ability of Q1 to reject all ions with an  $m/z \neq 86, 87$  and  $88$ ). Fig. 11 shows the isotopic pattern for a standard solution of Sr and the same solution spiked with otherwise interfering elements *i.e.*, Ag, Cd, Pd and Rb, using both SQ and MS/MS mode. It can be appreciated that there is spectral overlap when measuring on-mass using both modes and in the mass-shift ( $\text{SrF}^+$ ) approach in SQ mode, while in MS/MS mode, the isotopic pattern is preserved, thus allowing a direct isotopic analysis of Sr without prior Rb/Sr separation. In an earlier work performed with single quad ICP-DRC-QMS, matrix-matching of the standards used for mass bias correction was necessary.<sup>37</sup>

### 3.3. Hyphenated ICP-MS/MS applications

Like all ICP-MS devices, an ICP-tandem mass spectrometer can be used in combination with other sample introduction systems or separation techniques to improve the performance for some

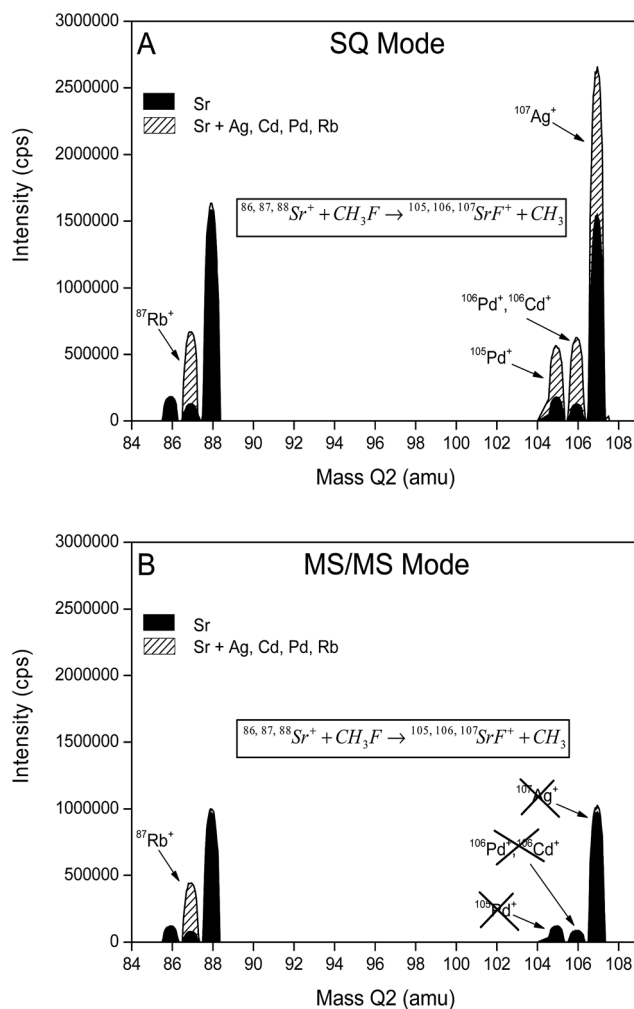


Fig. 11 Mass spectrum showing the isotopic composition of Sr at the original  $m/z$  (86, 87 and 88) and at the  $m/z$  of the selected reaction product ion ( $\text{SrF}^+$ , 105, 106 and 107) for a standard solution of Sr (black) and for a standard solution of Sr doped with Ag, Cd, Pd and Rb (dashed lines) in both, SQ (A) and MS/MS (B) mode. Adapted from Bolea-Fernandez *et al.*<sup>59</sup>

specific and/or more demanding applications. A brief review of some of these hyphenated ICP-MS/MS applications is presented in this section.

**3.3.1. Chromatography.** When coupling LC or GC to ICP-MS, speciation analysis can be performed with highly sensitive detection, while the setup provides the advantage of structure-independent quantification. As many of the elements typically of interest in speciation studies (*e.g.*, S, P, Cl, As, Se) are prone to spectral overlap in ICP-MS, the added value of using tandem mass spectrometry in this context is clear. Moreover, especially when combining LC and ICP-MS, the effluent of the LC system often contains a large fraction of organic solvents that may lead to additional interferences in the ICP-MS detection, which have to be tackled. Nelson *et al.*<sup>60</sup> developed a new strategy for the determination of organo-Cl, -P and -S compounds in pesticides by means of gas chromatography ICP-MS/MS (GC-ICP-MS/MS). In this work,  $^{31}\text{P}^+$  and  $^{32}\text{S}^+$  were measured simultaneously using the MS/MS mode with  $\text{O}_2$  as the

reaction gas selected to avoid spectral overlap by means of O-atom transfer, producing the corresponding  $^{31}\text{PO}^+$  and  $^{32}\text{SO}^+$  reaction product ions ( $m/z = 47$  and  $48$ , respectively). Cl, however, could not be measured under the same conditions due to the different reactivity of Cl towards  $\text{O}_2$  (charge transfer being the dominant process  $\text{Cl}^+ + \text{O}_2 \rightarrow \text{Cl} + \text{O}_2^+$ ). Thus, Cl was measured upon reaction with  $\text{H}_2$  in the CRC, according to the reaction pathway  $\text{Cl}^+ + \text{H}_2 \rightarrow \text{ClH}_2^+$ . It is important to stress that the chemical resolution of the spectral interferences affecting  $^{35}\text{Cl}^+$  by reaction with  $\text{H}_2$ , with formation and detection of  $^{35}\text{ClH}_2^+$ , can only be accomplished successfully in MS/MS mode, otherwise there would be overlap of the signals of  $^{35}\text{ClH}_2^+$  and  $^{37}\text{Cl}^+$ . Although also  $^{37}\text{Cl}$  reacts with  $\text{H}_2$  to form  $^{37}\text{ClH}_2^+$ , mass-shift reactions are typically not 100% efficient, such that part of the  $^{37}\text{Cl}$  ions are still detected at their original  $m/z = 37$ , as a consequence of which there is overlap with the  $^{35}\text{ClH}_2^+$  signal. By using both methods, interference-free conditions for the measurement of P, S and Cl were obtained with LODs of 0.0005, 0.7 and 0.1  $\mu\text{g kg}^{-1}$ , respectively. Also, the same approach for interference-free determination of Cl was evaluated by Klencsár *et al.*<sup>64</sup> A fast, accurate and precise method for the separation and determination of the total contents of drug-related Cl and Br in human blood plasma was developed. *Via* HPLC-ICP-MS/MS, Cl was measured as the corresponding  $^{35}\text{ClH}_2^+$  reaction product ion (mass-shift), while  $^{79}\text{Br}$  was measured at the original  $m/z$  (on-mass). As a proof-of-concept, blood plasma samples were analyzed, that have been obtained from a clinical study involving administration of a pharmaceutical compound containing the two target analytes to human volunteers. Successful cross-validation was performed *via* comparison of the results obtained for Cl and Br. Díez Fernández *et al.*<sup>62</sup> described a similar method for the determination of  $^{31}\text{P}$  and  $^{32}\text{S}$  in the context of absolute quantitative proteomics and phosphoproteomics *via* HPLC-ICP-MS/MS with absolute detection limits of 10 and 7 fmol for S and P, respectively.

HPLC-ICP-MS/MS has also been used for the speciation of different As-compounds at trace or ultra-trace levels ( $\text{As}^+ + \text{O}_2 \rightarrow \text{AsO}^+ + \text{O}$ ).<sup>63,64</sup> This approach was also used by Musil *et al.*<sup>65</sup> and compared with selective hydride generation (HG-ICP-MS/MS) for monitoring of inorganic As (iAs) in the context of food analysis. When using  $\text{NaBH}_4$  at acidic conditions (high HCl concentration), only iAs is converted into  $\text{AsH}_3$  and transferred to the gaseous phase, while organoarsenic compounds remained in the liquid phase. This method was shown faster than HPLC-ICP-MS/MS, without significant statistical difference for iAs concentration and with similar LODs.

A method for the accurate quantification of selenoproteins in plasma was developed by Deitrich *et al.*<sup>66</sup> The use of species-specific double isotope dilution mass spectrometry (SSIDA) was evaluated for the determination of protein-bound Se *via* HPLC-ICP-MS/MS. O-atom transfer ( $\text{SeO}^+$  selected as reaction product ion) was used to avoid the strong spectral overlap affecting Se isotopes. This approach minimized the impact of analyte losses and/or transformations during sample preparation and analysis. It enables for the determination of basal levels ( $\sim 60 \mu\text{g kg}^{-1}$  Se) and suffices for its use as biomarker for nutrition and disease, including cancer and Alzheimer's.

**3.3.2. Asymmetric flow field-flow fractionation.** Hyphenation of asymmetric flow field-flow fractionation to ICP-MS/MS (FFF-ICP-MS/MS) has been reported on in literature for nanoparticle analysis, *i.e.* separation and identification of nanoparticles. Menendez-Miranda *et al.*,<sup>67,68</sup> developed a method for the interference-free determination of Cd, S, Se and Zn aiming to assess the chemical composition of CdSe/ZnS quantum-dots populations (QDs). For such determination, a multi-element method was developed by combining on-mass and mass-shift approaches. It was shown that  $0.35 \text{ mL min}^{-1}$  of  $\text{O}_2$  suffices to convert  $^{32}\text{S}^+$  and  $^{80}\text{Se}^+$  ions into the corresponding  $\text{SO}^+$  and  $\text{SeO}^+$  reaction product ions ( $m/z = 48$  and  $96$ , respectively), while  $^{111}\text{Cd}^+$  and  $^{66}\text{Zn}^+$  do not show reactivity towards  $\text{O}_2$ .

Another example on the use of FFF-ICP-MS/MS is the work of Aureli *et al.*,<sup>69</sup> who aimed at the development of easy, reliable and sensitive analytical methods for the determination of nano-sized silica, thus enabling the evaluation of possible effects of synthetic amorphous silica in nanomaterials on human health. Si was measured free from spectral interference after conversion of  $\text{Si}^+$  ions into the corresponding  $\text{SiO}^+$  reaction product ions by adding  $\text{O}_2$  gas in the cell ( $m/z \text{ Q2} = 44, 45$  and  $46$  for  $^{28}\text{Si}$ ,  $^{29}\text{Si}$  and  $^{30}\text{Si}$ , respectively). The method was successfully applied to the characterization of a reference material and a Si-suspension, containing particles with nominal diameters of 20 and 140 nm, respectively.

In addition to  $\text{O}_2$ , also more reactive gases, such as  $\text{NH}_3$ , have been used in the analysis of nanoparticles. Soto-Alvaredo *et al.*<sup>70</sup> reported on the detection and characterization of  $\text{TiO}_2$  NPs *via* sedimentation field-flow fractionation (SdFFF) coupled to ICP-MS/MS. Ti isotopes were determined free from spectral overlap as their corresponding  $\text{Ti}(\text{NH}_3)_6^+$  reaction product ions. Although the results were affected for samples with high ionic strength (*e.g.*, sea water) owing to aggregation/agglomeration with subsequent sedimentation, in the case of samples with relatively low salt concentration (*e.g.*, lake water), the method developed was able to detect  $\text{TiO}_2$  NPs in the size range between  $\sim 75$  and  $400$  nm. These results open the possibility for the investigation of  $\text{TiO}_2$  NPs (and other oxide-based NPs) in environmental samples.

**3.3.3. Laser ablation.** The combination of laser ablation (LA) with ICP-MS detection is a powerful combination with as main advantage the possibility to directly analyze solid materials after limited sample preparation and with minimal sample damage. Moreover, by coupling LA to ICP-MS, the application range of ICP-MS is extended to spatially resolved analysis of selected sample regions. To date, only a few LA-ICP-MS/MS papers have been published. This may be related to the fact that the LA unit provides transient signals, while – due to the double mass selection – ICP-MS/MS can be seen as a somewhat slower detector than single quadrupole ICP-MS instruments.

Bishop *et al.*<sup>71</sup> evaluated the capabilities of LA-ICP-MS/MS for elemental bio-imaging (EBI) of trace metal distributions in tissue sections. Different modes of operation were evaluated: no gas, bandpass ( $\text{H}_2$  in the CRC) and MS/MS ( $\text{O}_2$  in the CRC). The best conditions were found when using  $\text{O}_2$  and this approach was used for evaluating the distribution of Zn (on-mass) within

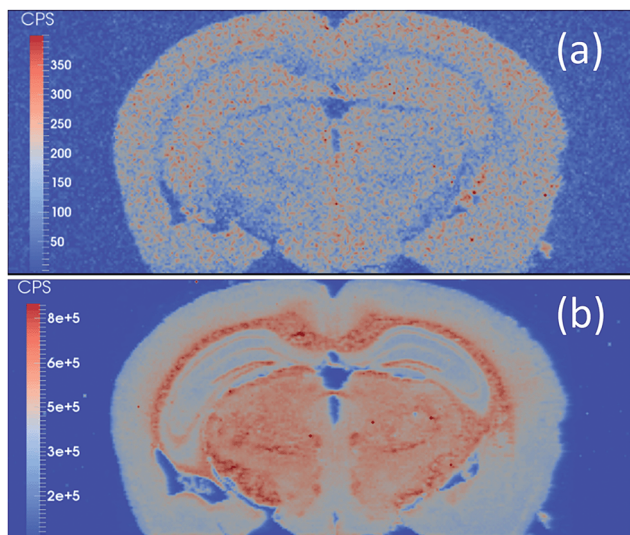


Fig. 12 Image of a mouse brain obtained with LA-ICP-MS/MS ( $O_2$  mode). (a)  $^{80}Se^{16}O^+ \rightarrow ^{80}Se^{16}O^+$  and (b)  $^{31}P^{16}O^+ \rightarrow ^{31}P^{16}O^+$ . Adapted from Bishop *et al.*<sup>71</sup>

prostate cancer biopsy sample and of P and Se (mass-shift –  $PO^+$  and  $SeO^+$ ) in a mouse brain (Fig. 12). This work was the first to demonstrate the potential of LA-ICP-MS/MS for EBI.

Bolea-Fernandez *et al.*<sup>72</sup> reported on the use of LA-ICP-MS/MS for direct Sr isotopic analysis of solid samples with high Rb/Sr ratio. The approach used in this work involves chemical resolution of the isobaric overlap of the signals of  $^{87}Rb$  and  $^{87}Sr$  *via* reaction with  $CH_3F$  (as described in Section 3.2.2 for digested materials), enabling accurate isotopic analysis of Sr without previous separation from Rb for samples showing high Rb/Sr ratio. A systematic comparison revealed that the use of wet plasma conditions, obtained by mixing of the LA aerosol with nebulized  $H_2O$ , provided better accuracy and precision (<0.05% RSD) than did dry plasma conditions. NIST SRM 610 glass was used as the external standard for mass bias correction; no closer matrix-matching was required. This methodology can be seen as a good and fast alternative for real-life applications in which the differences in isotopic composition between different samples are not too small, and for pre-screening and pre-selecting samples for higher-precision isotopic analysis, *i.e.* using TIMS or MC-ICP-MS.

#### 4. Summary and future perspectives

In this chapter, the operating principles of ICP-MS/MS have been described with the focus on the differences between the ICP-MS/MS configuration and conventional quadrupole-based ICP-MS. The use of ICP-MS/MS opens new possibilities to deal with spectral overlap by offering superior control over the cell chemistry, thus enhancing the possibilities of chemical resolution in ICP-QMS. The different scanning options are powerful tools for method development and for identification of the best suited reaction product ions, even or especially when using highly reactive gases. Furthermore, some demanding

applications, covering a wide range of application fields, have been shortly reviewed. From this, the reader should have a clear view on the general capabilities and limitations of ICP-tandem mass spectrometry. The fast increase in the number of ICP-MS/MS papers in literature illustrates these added values. Nevertheless, the technique is still young and it is expected that over the next years, many more application areas will benefit from the additional possibilities offered by ICP-MS/MS.

#### References

- 1 E. H. Evans and J. J. Giglio, *J. Anal. At. Spectrom.*, 1993, **8**, 1–18.
- 2 R. F. J. Dams, J. Goossens and L. Moens, *Mikrochim. Acta*, 1995, **119**, 277–286.
- 3 T. W. May and R. H. Wiedmeyer, *At. Spectrosc.*, 1998, **19**, 150–155.
- 4 K. Sakata and K. Kawabata, *Spectrochim. Acta, Part B*, 1994, **49**, 1027–1038.
- 5 M. G. Minnich and R. S. Houk, *J. Anal. At. Spectrom.*, 1998, **13**, 167–174.
- 6 S. D. Tanner, *J. Anal. At. Spectrom.*, 1995, **10**, 905–921.
- 7 N. Jakubowski, L. Moens and F. Vanhaecke, *Spectrochim. Acta, Part B*, 1998, **53**, 1739–1763.
- 8 L. Moens and N. Jakubowski, *Anal. Chem.*, 1998, **70**, 251A–256A.
- 9 N. Jakubowski, T. Prohaska, L. Rottmann and F. Vanhaecke, *J. Anal. At. Spectrom.*, 2011, **26**, 693–726.
- 10 J. T. Rowan and R. S. Houk, *Appl. Spectrosc.*, 1989, **43**, 976–980.
- 11 D. J. Douglas, *Can. J. Spectrosc.*, 1989, **34**, 38–49.
- 12 S. D. Tanner and V. I. Baranov, *At. Spectrosc.*, 1999, **20**, 45–52.
- 13 S. D. Tanner, V. I. Baranov and D. R. Bandura, *Spectrochim. Acta, Part B*, 2002, **57**, 1361–1452.
- 14 V. I. Baranov and S. D. Tanner, *J. Anal. At. Spectrom.*, 1999, **14**, 1133–1142.
- 15 N. Yamada, *Spectrochim. Acta, Part B*, 2015, **110**, 31–44.
- 16 I. Feldmann, N. Jakubowski and D. Stuewer, *Fresenius. J. Anal. Chem.*, 1999, **364**, 415–421.
- 17 I. Feldmann, N. Jakubowski, C. Thomas and D. Stuewer, *Fresenius. J. Anal. Chem.*, 1999, **365**, 422–428.
- 18 S. D. Tanner, V. I. Baranov and U. Vollkopf, *J. Anal. At. Spectrom.*, 2000, **15**, 1261–1269.
- 19 S. D. Tanner and V. I. Baranov, *J. Am. Soc. Mass Spectrom.*, 1999, **10**, 1083–1094.
- 20 L. Balcaen, E. Bolea-Fernandez, M. Resano and F. Vanhaecke, *Anal. Chim. Acta*, 2015, **894**, 7–19.
- 21 T.-S. Lum and K. S.-Y. Leung, *J. Anal. At. Spectrom.*, 2016, **31**, 1078–1088.
- 22 K. K. Murray, R. K. Boyd, M. N. Eberlin, G. J. Langley, L. Li and Y. Naito, *Pure Appl. Chem.*, 2013, **85**, 1515–1609.
- 23 Z. Du, T. N. Olney and D. J. Douglas, *J. Am. Soc. Mass Spectrom.*, 1997, **8**, 1230–1236.
- 24 S. F. Boulyga and S. Becker, *J. Anal. At. Spectrom.*, 2002, **17**, 1202–1206.

- 25 K. Blaum, C. Geppert, P. Müller, W. Nörtershäuser, K. Wendt and B. A. Bushaw, *Int. J. Mass Spectrom.*, 2000, **202**, 81–89.
- 26 A. Virgilio, R. S. Amais, C. D. B. Amaral, L. L. Fialho, D. Schiavo and J. A. Nóbrega, *Spectrochim. Acta, Part B*, 2016, **126**, 31–36.
- 27 J. Goossens, F. Vanhaecke, L. Moens and R. Dams, *Anal. Chim. Acta*, 1993, **280**, 137–143.
- 28 J. Darrouzès, M. Bueno, G. Lespès and M. Potin-Gautier, *Talanta*, 2007, **71**, 2080–2084.
- 29 S. Meyer, M. Matissek, S. M. Müller, M. S. Taleshi, F. Ebert, K. A. Francesconi and T. Schwerdtle, *Metallomics*, 2014, **6**, 1023–1033.
- 30 S. Meyer, J. Schulz, A. Jeibmann, M. S. Taleshi, F. Ebert, K. A. Francesconi and T. Schwerdtle, *Metallomics*, 2014, **6**, 2010–2014.
- 31 L. Balcaen, G. Woods, M. Resano and F. Vanhaecke, *J. Anal. At. Spectrom.*, 2013, **28**, 33–39.
- 32 X.-w. Wang, J.-f. Liu, X.-y. Wang, B. Shao, L.-p. Liu and J. Zhang, *Anal. Methods*, 2015, **7**, 3224–3228.
- 33 D. P. Bishop, D. J. Hare, F. Fryer, R. V. Taudte, B. R. Cardoso, N. Cole and P. A. Doble, *Analyst*, 2015, **140**, 2842–2846.
- 34 N. Sugiyama and Y. Shikamori, *J. Anal. At. Spectrom.*, 2015, **30**, 2481–2487.
- 35 K. Böting, S. Treu, P. Leonhard, C. Heiß and N. H. Bings, *J. Anal. At. Spectrom.*, 2014, **29**, 578–582.
- 36 L. Balcaen, E. Bolea-Fernandez, M. Resano and F. Vanhaecke, *Anal. Chim. Acta*, 2014, **809**, 1–8.
- 37 L. J. Moens, F. F. Vanhaecke, D. R. Bandura, V. I. Baranov and S. D. Tanner, *J. Anal. At. Spectrom.*, 2001, **16**, 991–994.
- 38 N. Nonose, M. Ohata, T. Narukawa, A. Hioki and K. Chiba, *J. Anal. At. Spectrom.*, 2009, **24**, 310–319.
- 39 X. Zhao, G. K. Koyanagi and D. K. Bohme, *J. Phys. Chem. A*, 2006, **110**, 10607–10618.
- 40 P. Redondo, A. Varela-Álvarez, V. M. Rayón, A. Largo, J. A. Sordo and C. Barrientos, *J. Phys. Chem. A*, 2013, **117**, 2932–2943.
- 41 E. Bolea-Fernandez, L. Balcaen, M. Resano and F. Vanhaecke, *Anal. Bioanal. Chem.*, 2015, **407**, 919–929.
- 42 C. D. B. Amaral, R. S. Amais, L. L. Fialho, D. Schiavo, T. Amorim, A. R. A. Nogueira, F. R. P. Rocha and J. A. Nóbrega, *Anal. Methods*, 2015, **7**, 1215–1220.
- 43 S. Diez Fernández, J. Ruiz Encinar, A. Sanz-Medel, D. Isensee and H. M. Stoll, *Geochem., Geophys., Geosyst.*, 2015, **16**, 2005–2014.
- 44 R. S. Amais, A. Virgilio, D. Schiavo and J. A. Nóbrega, *Microchem. J.*, 2015, **120**, 64–68.
- 45 R. C. Machado, C. D. B. Amaral, D. Schiavo, J. A. Nóbrega and A. R. A. Nogueira, *Microchem. J.*, 2017, **130**, 271–275.
- 46 T. Suoranta, S. N. H. Bokhari, T. Meisel, M. Niemelä and P. Perämäki, *Geostand. Geoanal. Res.*, 2016, **40**, 559–569.
- 47 E. Bolea-Fernandez, L. Balcaen, M. Resano and F. Vanhaecke, *Anal. Chem.*, 2014, **86**, 7969–7977.
- 48 E. Bolea-Fernandez, K. Phan, L. Balcaen, M. Resano and F. Vanhaecke, *Anal. Chim. Acta*, 2016, **941**, 1–9.
- 49 P. Rodríguez-González, J. M. Marchante-Gayón, J. I. Garcia Alonso and A. Sanz-Medel, *Spectrochim. Acta, Part B*, 2005, **60**, 151–207.
- 50 L. Bamonti, S. Theiner, N. Rohr-Udilova, B. K. Keppler and G. Koellensperger, *J. Anal. At. Spectrom.*, 2016, **31**, 2227–2232.
- 51 T. Ohno, Y. Muramatsu, Y. Shikamori, C. Toyama, N. Okabe and H. Matsuzaki, *J. Anal. At. Spectrom.*, 2013, **28**, 1283–1287.
- 52 T. Ohno and Y. Muramatsu, *J. Anal. At. Spectrom.*, 2014, **29**, 347–351.
- 53 J. Zheng, W. Bu, K. Tagami, Y. Shikamori, K. Nakano, S. Uchida and N. Ishii, *Anal. Chem.*, 2014, **86**, 7103–7110.
- 54 J. Zheng, K. Tagami, W. Bu, S. Uchida, Y. Watanabe, Y. Kubota, S. Fuma and S. Ihara, *Environ. Sci. Technol.*, 2014, **48**, 5433–5438.
- 55 G. Yang, H. Tazoe and M. Yamada, *Sci. Rep.*, 2016, DOI: 10.1038/srep24119.
- 56 J. Zheng, L. Cao, K. Tagami and S. Uchida, *Anal. Chem.*, 2016, **88**, 8772–8779.
- 57 G. Yang, H. Tazoe and M. Yamada, *Anal. Chim. Acta*, 2016, **908**, 177–184.
- 58 L. Cao, J. Zheng, H. Tsukada, S. Pan, Z. Wang, K. Tagami and S. Uchida, *Talanta*, 2016, **159**, 55–63.
- 59 E. Bolea-Fernandez, L. Balcaen, M. Resano and F. Vanhaecke, *J. Anal. At. Spectrom.*, 2016, **31**, 303–310.
- 60 J. Nelson, H. Hopfer, F. Silva, S. Wilbur, J. Chen, K. S. Ozawa and P. L. Wylie, *J. Agric. Food Chem.*, 2015, **63**, 4478–4483.
- 61 B. Klencsár, E. Bolea-Fernandez, M. R. Flórez, L. Balcaen, F. Cuyckens, F. Lynen and F. Vanhaecke, *J. Pharm. Biomed. Anal.*, 2016, **124**, 112–119.
- 62 S. Diez Fernández, N. Sugishama, J. Ruiz Encinar and A. Sanz-Medel, *Anal. Chem.*, 2012, **84**, 5851–5857.
- 63 J. D. Palcic, J. S. Jones, E. L. Flagg and S. F. Donovan, *J. Anal. At. Spectrom.*, 2015, **30**, 1799–1808.
- 64 B. P. Jackson, *J. Anal. At. Spectrom.*, 2015, **30**, 1405–1407.
- 65 S. Musil, A. H. Pétursdóttir, A. Raab, H. Gunnlaugsdóttir, E. Krupp and J. Feldmann, *Anal. Chem.*, 2014, **86**, 993–999.
- 66 C. L. Deitrich, S. Cuello-Nuñez, D. Kmiotek, F. A. Torma, M. E. del Castillo Busto, P. Fisicaro and H. Goenaga-Infante, *Anal. Chem.*, 2016, **88**, 6357–6365.
- 67 M. Menendez-Miranda, M. T. Fernandez-Arguelles, J. M. Costa-Fernandez, J. Ruiz Encinar and A. Sanz-Medel, *Anal. Chim. Acta*, 2014, **839**, 8–13.
- 68 M. Menendez-Miranda, J. Ruiz Encinar, J. M. Costa-Fernandez and A. Sanz-Medel, *J. Chromatogr. A*, 2015, **1422**, 247–252.
- 69 F. Aureli, M. D'Amato, A. Raggi and F. Cubadda, *J. Anal. At. Spectrom.*, 2015, **30**, 1266–1273.
- 70 J. Soto-Alvaredo, F. Dutschke, J. Bettmer, M. Montes-Bayón, D. Pröfrock and A. Prange, *J. Anal. At. Spectrom.*, 2016, **31**, 1549–1555.
- 71 D. P. Bishop, D. Clases, F. Fryer, E. Williams, S. Wilkins, D. J. Hare, N. Cole, W. Karst and P. A. Doble, *J. Anal. At. Spectrom.*, 2016, **31**, 197–202.

- 72 E. Bolea-Fernandez, S. J. M. Van Malderen, L. Balcaen, M. Resano and F. Vanhaecke, *J. Anal. At. Spectrom.*, 2016, **31**, 464–472.
- 73 P. Kumkrong, B. Thiensong, P. M. Le, G. McRae, A. Windust, S. Deawtong, J. Meija, P. Maxwell, L. Yang and Z. Mester, *Anal. Chim. Acta*, 2016, **943**, 41–49.
- 74 B. O. Jackson, A. Liba and J. Nelson, *J. Anal. At. Spectrom.*, 2015, **30**, 1179–1183.
- 75 F. C. Pinheiro, C. D. B. Amaral, D. Schiavo and J. A. Nóbrega, *Food Analytical Methods*, 2016, DOI: 10.1007/s12161-12016-10663-12167.
- 76 S. Meyer, G. Raber, F. Ebert, L. Leffers, S. M. Müller, M. S. Taleshi, K. A. Francesconi and T. Schwerdtle, *Toxicol. Res.*, 2015, **4**, 1289–1296.
- 77 X. Hu, Z. Cao, W. Sun, H. Yang, P. Xu and Z. Zhu, *Anal. Methods*, 2016, **8**, 6150–6157.
- 78 R. S. Pappas, N. Matone, N. Gonzalez-Jimenez, M. R. Fresquez and C. H. Watson, *J. Anal. Toxicol.*, 2015, **39**, 347–352.
- 79 C. Walkner, R. Gratzer, T. Meisel and S. N. H. Bokhari, *Org. Geochem.*, 2016, **103**, 22–30.
- 80 R. S. Pappas, N. Gray, N. Gonzalez-Jimenez, M. Fresquez and C. H. Watson, *J. Anal. Toxicol.*, 2015, 1–5.
- 81 F. Ebert, S. Meyer, L. Leffers, G. Raber, K. A. Francesconi and T. Schwerdtle, *J. Trace Elem. Med. Biol.*, 2016, **38**, 150–156.
- 82 E. R. Pereira, J. F. Kopp, A. Raab, E. M. Krupp, J. d. C. Menoyo, E. Carasek, B. Welz and J. Feldmann, *J. Anal. At. Spectrom.*, 2016, **31**, 1836–1845.
- 83 Y. Koehler, E. M. Luther, S. Meyer, T. Schwerdtle and R. Dringen, *J. Trace Elem. Med. Biol.*, 2014, **28**, 328–337.
- 84 A. H. Pétursdóttir, N. Friedrich, S. Musil, A. Raab, H. Gunnlaugsdóttir, E. Krupp and J. Feldmann, *Anal. Methods*, 2014, **6**, 5392–5396.
- 85 C. D. Amaral, R. S. Amais, L. L. Fialho, D. Schiavo, A. R. A. Nogueira and J. A. Nóbrega, *Microchem. J.*, 2015, **122**, 29–32.
- 86 K. J. Hogmalm, T. Zack, A. K.-O. Karlsson, A. S. L. Sjöqvist and D. Garbe-Schönberg, *J. Anal. At. Spectrom.*, 2016, **32**, 305–313.
- 87 A. R. Montoro Bustos, M. Garcia-Cortes, H. González-Iglesias, J. Ruiz Encinar, J. M. Costa-Fernández, M. Coca-Prados and A. Sanz-Medel, *Anal. Chim. Acta*, 2015, **879**, 77–84.
- 88 A. Santoro, V. Thoss, S. R. Guevara, D. Urgast, A. Raab, S. Mastrolitti and J. Feldmann, *Appl. Radiat. Isot.*, 2015, **107**, 323–329.
- 89 L. Somoano-Blanco, P. Rodríguez-González, D. Pröfrock, A. Prange and J. I. Garcia Alonso, *Anal. Methods*, 2015, **7**, 9068–9075.
- 90 D. J. Hare, E. P. Raven, B. R. Roberts, M. Bogeski, S. D. Portbury, C. A. McLean, C. L. Masters, J. R. Connor, A. I. Bush, P. J. Crouch and P. A. Doble, *NeuroImage*, 2016, **137**, 124–131.
- 91 D. Bouzas-Ramos, M. Menéndez-Miranda, J. M. Costa-Fernández, J. Ruiz Encinar and A. Sanz-Medel, *RSC Adv.*, 2016, **6**, 19964–19972.
- 92 Y. Muramatsu, H. Matsuzaki, C. Toyama and T. Ohno, *J. Environ. Radioact.*, 2015, **139**, 344–350.
- 93 R. S. Amais, C. D. B. Amaral, L. L. Fialho, D. Schiavo and J. A. Nóbrega, *Anal. Methods*, 2014, **6**, 4516–4520.
- 94 J. Gong, M. J. Solivio, E. J. Merino, J. A. Caruso and J. A. Landero-Figueroa, *Anal. Bioanal. Chem.*, 2015, **407**, 2433–2437.
- 95 S. Theiner, C. Kornauth, H. P. Vabanov, M. Galanski, S. V. Schoonhoven, P. Heffeter, W. Berger, A. E. Egger and B. K. Keppler, *Metallomics*, 2015, **7**, 1256–1264.
- 96 S. Theiner, E. Schreiber-Brynzak, M. A. Jakupec, M. Galanski, G. Koellensperger and B. K. Keppler, *Metallomics*, 2016, **8**, 398–402.
- 97 A. Brandt-Kjelsen, E. Govasmark, A. Haug and B. Salbu, *J. Anim. Physiol. Anim. Nutr.*, 2014, **98**, 547–558.
- 98 S. Cueto Diaz, J. Ruiz Encinar and J. I. Garcia Alonso, *Anal. Chim. Acta*, 2014, **844**, 48–53.
- 99 H.-S. Lee, S. H. Kim, J.-S. Jeong, Y.-M. Lee and Y.-H. Yim, *Metrologia*, 2015, **52**, 619–627.
- 100 G. Hermann, L. H. Møller, B. Gammelgaard, J. Hohlweg, D. Mattanovich, S. Hann and G. Koellensperger, *J. Anal. At. Spectrom.*, 2016, **31**, 1830–1835.
- 101 F. Calderón-Celis, S. Diez-Fernández, J. M. Costa-Fernández, J. Ruiz Encinar, J. J. Calvete and A. Sanz-Medel, *Anal. Chem.*, 2016, **88**, 9699–9706.
- 102 L. Whitty-Lévilé, E. Drouin, M. Constantin, C. Bazin and D. Larivière, *Spectrochim. Acta, Part B*, 2016, **118**, 112–118.
- 103 A. F. Oliveira, J. Landero, K. Kubachka, A. R. A. Nogueira, M. A. Zanetti and J. Caruso, *J. Anal. At. Spectrom.*, 2016, **31**, 1034–1040.
- 104 K. M. Kubachka, T. Hanley, M. Mantha, R. A. Wilson, T. M. Falconer, Z. Kassa, A. Oliveira, J. Landero and J. Caruso, *Food Chem.*, 2016, **218**, 313–320.
- 105 Y. Anan, Y. Hatakeyama, M. Tokumoto and Y. Ogra, *Anal. Sci.*, 2013, **29**, 787–792.
- 106 G. Alkiviadis, D. Thomas, B. Evelyne, J. Patrick, G. Stephane, B. Sylvain and C. Charlotte, *Anal. Chim. Acta*, 2016, **954**, 68–76.
- 107 T. Zack and K. J. Hogmalm, *Chem. Geol.*, 2016, **437**, 120–133.
- 108 A. M. Cruz-Urbe, R. Mertz-Kraus, T. Zack, M. D. Feineman, G. Woods and D. E. Jacob, *Geostand. Geoanal. Res.*, 2016, DOI: 10.1111/ggr.12132.
- 109 M. Tanimizu, N. Sugiyama, E. Ponzevera and G. Bayon, *J. Anal. At. Spectrom.*, 2013, **28**, 1372–1376.
- 110 G. Yang, H. Tazoe and M. Yamada, *Anal. Chim. Acta*, 2016, **944**, 44–50.